CHAPTER 5

Perturbation Theory

5.1 INTRODUCTION: THE VAN DER WAALS MODEL

The intermolecular pair potential often separates in a natural way into two parts: a harsh, short-range repulsion and a smoothly varying, long-range attraction. A separation of this type is an explicit ingredient of many empirical representations of the intermolecular forces, including the Lennard-Jones potential. It is now generally accepted that the structure of most simple liquids, at least at high density, is largely determined by the way in which the molecular hard cores pack together. By contrast, the attractive interactions may, in a first approximation, be regarded as giving rise to a uniform background potential that provides the cohesive energy of the liquid but has little effect on its structure. A further plausible approximation consists in modelling the short-range forces by the infinitely steep repulsion of the hard-sphere potential. The properties of the liquid of interest can in this way be related to those of a hard-sphere reference system, the attractive part of the potential being treated as a perturbation. The choice of the hard-sphere fluid as a reference system is an obvious one, since its thermodynamic and structural properties are well known.

The idea of representing a liquid as a system of hard spheres moving in a uniform, attractive potential is an old one, providing as it does the physical basis for the famous van der Waals equation of state. At the time of van der Waals, little was known of the properties of the dense hard-sphere fluid. The approximation that van der Waals made was to take the excluded volume per sphere of diameter d as equal to $\frac{2}{3}\pi d^3$ (or four times the hard-sphere volume), which leads to an equation of state of the form

$$\frac{\beta P_0}{\rho} = \frac{1}{1-4\eta} \tag{5.1.1}$$

where, as before, η is the packing fraction. Equation (5.1.1) gives the second virial coefficient correctly (see (3.9.14)), but it fails badly at high densities. In particular, the pressure diverges as $\eta \to 0.25$, a packing fraction lying well below that of the fluid–solid transition ($\eta \approx 0.49$).

Considerations of thermodynamic consistency[1] show that the equation of state compatible with the hypothesis of a uniform, attractive background is necessarily of the form

$$\frac{\beta P}{\rho} = \frac{\beta P_0}{\rho} - \beta\rho a \tag{5.1.2}$$

where a is a positive constant; this is equivalent to supposing that the chemical potential is lowered with respect to that of the hard spheres by an amount proportional to the density and equal to $2a\rho$. The classic van der Waals equation is then recovered by substituting for P_0 from (5.1.1). It is clear that a first step towards improving on van der Waals's result is to replace (5.1.1) by a more accurate hard-sphere equation of state, such as that of Carnahan and Starling, (3.9.17). A calculation along these lines was first carried out by Longuet-Higgins and Widom,[2] who thereby were able to account successfully for the melting properties of rare-gas solids.

The sections that follow are devoted to perturbation methods that may be regarded as attempts to improve the theory of van der Waals in a systematic fashion. The methods we describe have as a main ingredient the assumption that the structure of a dense, monatomic fluid resembles that of an assembly of hard spheres. Justification for this intuitively appealing idea is provided by the great success of the perturbation theories to which it gives rise, and which mostly reduce to (5.1.2) in some well-defined limit, but more direct evidence exists to support it. For example, it has long been known[3] that the experimental structure factors of a variety of liquid metals near their normal melting points can to a good approximation be superimposed on the structure factor of an "equivalent" hard-sphere fluid, and Figure 5.1 shows the results of a similar but more elaborate analysis of data obtained by molecular-dynamics calculations for the Lennard-Jones fluid. The fact that the attractive forces play such an apparently minor role in these examples is understandable through the following argument.[4] Equation (3.6.9) shows that the structure factor determines the density response of the fluid to a weak, external field. If the external potential is identified with the potential due to a test particle placed at the origin, the long-range part of that potential gives rise to a long-wavelength response in the density. In the long-wavelength limit ($k \to 0$), the response is proportional to $S(k = 0)$ and hence, through (3.6.11), to the compressibility. Under triple-point conditions the compressibility of a liquid is very small: typically the ratio of χ_T to its ideal-gas value is approximately 0.02. The effects of long-wavelength perturbations are therefore greatly reduced. At lower densities, particularly in the

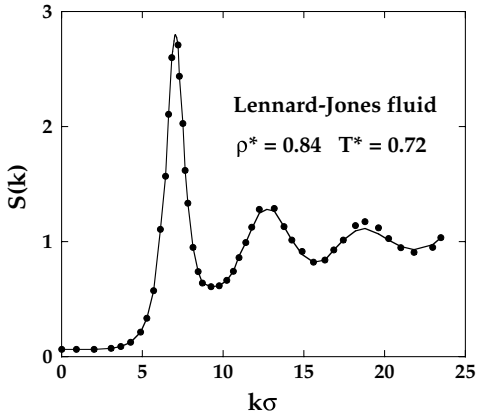

FIG. 5.1. Structure factor of the Lennard-Jones fluid close to the triple point (curve) and its representation by a hard-sphere model (points). After Verlet.[4]

critical region, the compressibility can become very large. The role of the attractive forces is then important and the simple van der Waals model no longer has a sound physical basis.

We shall assume throughout this chapter that the interactions between particles are pairwise additive, though there is no difficulty in principle in extending the treatment to include three-body and higher-order forces. We also suppose that the system of interest is homogeneous. The basis of all the perturbation theories we discuss is a division of the pair potential of the form

$$v(1,2) = v_0(1,2) + w(1,2) \tag{5.1.3}$$

where $v_0(1,2)$ is the pair potential of the reference system and $w(1,2)$ is the perturbation. The calculation then usually proceeds in two stages. The first step is to compute the effects of the perturbation on the thermodynamic properties and pair distribution function of the reference system. This can be done systematically via an expansion in powers either of inverse temperature (the "λ-expansion") or of a parameter that measures the range of the perturbation (the "γ-expansion"). When hard spheres themselves are the reference system, this completes the calculation, but in the more general situation the properties of some "soft-core" reference system must in turn be related to those of the hard-sphere fluid.

5.2 THE λ-EXPANSION

Consider a pair potential $v_\lambda(1,2)$ of the form

$$v_\lambda(1,2) = v_{\lambda_0}(1,2) + w_\lambda(1,2) \tag{5.2.1}$$

where λ is a parameter that varies between λ_0 and λ_1. When $\lambda = \lambda_0$, w_λ vanishes and the potential $v_{\lambda_0} \equiv v_0$ reduces to that of a reference system, the properties of which are assumed to be known, whereas for $\lambda = \lambda_1$ the potential $v_{\lambda_0} \equiv v$ is the one that characterises the system of interest. The quantity λ has the meaning of a coupling parameter: the effect of varying λ continuously from λ_0 to λ_1 is that of gradually increasing the perturbation $w_\lambda(1,2)$. The commonest example of such a potential is

$$v_\lambda(1,2) = v_0(1,2) + \lambda w(1,2) \tag{5.2.2}$$

with $\lambda_0 = 0$ and $\lambda_1 = 1$; when $\lambda = 1$, the potential is the same as that introduced in (5.1.3).

Let $V_N(\lambda)$, given by

$$V_N(\lambda) = \sum_{i=1}^{N} \sum_{j>i}^{N} v_\lambda(i,j) \tag{5.2.3}$$

be the total potential energy of a system of particles interacting through the potential (5.2.1). From the definitions of the configuration integral, (2.3.13), and the excess free energy (here denoted simply by F), (2.3.20), it follows immediately that the derivative of $F(\lambda)$ with respect to the coupling parameter is

$$\beta \frac{\partial F(\lambda)}{\partial \lambda} = \frac{1}{Z_N(\lambda)} \int \exp\bigl[-\beta V_N(\lambda)\bigr] \beta V_N'(\lambda)\, \mathrm{d}\mathbf{r}^N = \beta \bigl\langle V_N'(\lambda) \bigr\rangle_\lambda \tag{5.2.4}$$

where $V_N'(\lambda) \equiv \partial V_N(\lambda)/\partial\lambda$ and $\langle\cdots\rangle_\lambda$ denotes a canonical ensemble average for the system characterised by the potential $v_\lambda(1,2)$. Integration of (5.2.4) gives

$$\beta F(\lambda_1) = \beta F_0 + \beta \int_{\lambda_0}^{\lambda_1} \langle V_N'(\lambda)\rangle_\lambda \, \mathrm{d}\lambda \tag{5.2.5}$$

where $F_0 \equiv F_{\lambda_0}$ is the excess free energy of the reference system. A series expansion of the ensemble average $\langle V_N'(\lambda)\rangle_\lambda$ can now be made around its value for $\lambda = \lambda_0$:

$$\langle V_N'(\lambda)\rangle_\lambda = \langle V_N'(\lambda)\rangle_{\lambda_0} + (\lambda - \lambda_0)\frac{\partial}{\partial\lambda}\langle V_N'(\lambda)\rangle_\lambda\Big|_{\lambda=\lambda_0} + \mathcal{O}(\lambda-\lambda_0)^2 \tag{5.2.6}$$

The derivative with respect to λ in (5.2.6) is

$$\frac{\partial}{\partial\lambda}\langle V_N'(\lambda)\rangle_\lambda = \langle V_N''(\lambda)\rangle_\lambda - \beta\big(\langle[V_N'(\lambda)]^2\rangle_\lambda - \langle V_N'(\lambda)\rangle_\lambda^2\big) \tag{5.2.7}$$

and insertion of this result in (5.2.5) yields an expansion of the free energy in powers of $(\lambda_1 - \lambda_0)$:

$$\begin{aligned}\beta F(\lambda_1) = {} & \beta F_0 + (\lambda_1-\lambda_0)\beta\langle V_N'(\lambda_0)\rangle_{\lambda_0} \\ & + \tfrac{1}{2}(\lambda_1-\lambda_0)^2\big(\beta\langle V_N''(\lambda_0)\rangle_{\lambda_0} - \beta^2\big(\langle[V_N'(\lambda_0)]^2\rangle_{\lambda_0} - \langle V_N'(\lambda_0)\rangle_{\lambda_0}^2\big)\big) \\ & + \mathcal{O}(\lambda_1-\lambda_0)^3\end{aligned} \tag{5.2.8}$$

We now restrict ourselves to the important special case when $v_\lambda(1,2)$ is given by (5.2.2). If we define the total perturbation energy for $\lambda = 1$ as

$$W_N = \sum_{i=1}^{N}\sum_{j>i}^{N} w(i,j) \tag{5.2.9}$$

then $V_N' = W_N$, $V_N'' = 0$ and (5.2.8) simplifies to give

$$\beta F = \beta F_0 + \beta\langle W_N\rangle_0 - \tfrac{1}{2}\beta^2\big(\langle W_N^2\rangle_0 - \langle W_N\rangle_0^2\big) + \mathcal{O}\big(\beta^3\big) \tag{5.2.10}$$

The series (5.2.10) is called the *high-temperature expansion*, but the name is not entirely appropriate. Although successive terms are multiplied by increasing powers of β, the ensemble averages are also, in general, functions of temperature. However, when the reference system is a hard-sphere fluid, the averages depend only on density and the λ-expansion reduces to a Taylor series in T^{-1}. Equation (5.2.10) was first derived by Zwanzig,[5] who showed that the nth term in the series can be written in terms of the mean fluctuations $\langle[(W_N - \langle W_N\rangle_0)]^\nu\rangle_0$, with $\nu \leqslant n$. Thus every term in the expansion corresponds to a statistical average evaluated in the reference-system ensemble. The third and

fourth-order terms, for example, are

$$\begin{aligned}\beta F_3 &= \frac{\beta^3}{3!}\langle\big[W_N - \langle W_N\rangle_0\big]^3\rangle_0 \\ \beta F_4 &= -\frac{\beta^4}{4!}\big(\langle\big[W_N - \langle W_N\rangle_0\big]^4\rangle_0 - 3\langle\big[W_N - \langle W_N\rangle_0\big]^2\rangle_0^2\big)\end{aligned} \tag{5.2.11}$$

The assumption of pairwise additivity of the potential (including the perturbation) means that (5.2.5) can be written as

$$\frac{\beta F}{N} = \frac{\beta F_0}{N} + \frac{\beta}{2N}\int_0^1 \mathrm{d}\lambda \iint \rho_\lambda^{(2)}(1,2)w(1,2)\,\mathrm{d}1\,\mathrm{d}2 \tag{5.2.12}$$

where $\rho_\lambda^{(2)}(1,2)$ is the pair density for the system with potential $v_\lambda(1,2)$; this is a special case of the general result contained in (3.4.10). The pair density can then be expanded in powers of λ:

$$\rho_\lambda^{(2)}(1,2) = \rho_0^{(2)}(1,2) + \lambda\frac{\partial\rho_\lambda^{(2)}(1,2)}{\partial\lambda}\bigg|_{\lambda=0} + \mathcal{O}(\lambda^2) \tag{5.2.13}$$

When this result is inserted in (5.2.12) the term of zeroth order in λ yields the first-order term in the high-temperature expansion of the free energy:

$$\frac{\beta F_1}{N} = \frac{\beta}{2N}\iint \rho_0^{(2)}(1,2)w(1,2)\,\mathrm{d}1\,\mathrm{d}2 = \frac{\beta\rho}{2}\int g_0(1,2)w(1,2)\,\mathrm{d}\mathbf{r}_{12} \tag{5.2.14}$$

In this approximation the structure of the fluid is unaltered by the perturbation. At second order in λ, however, calculation of the free energy involves the derivative $\partial\rho_\lambda^{(2)}/\partial\lambda$. Care is needed in passing to the thermodynamic limit and the differentiation is easier to perform in the grand canonical ensemble. The final result for a closed system[6] is

$$\begin{aligned}\frac{\beta F_2}{N} = -\frac{\beta^2}{2}\Bigg(&\frac{\rho}{2}\int g_0(1,2)\big[w(1,2)\big]^2\,\mathrm{d}2 \\ &+ \rho^2\iint g_0^{(3)}(1,2,3)w(1,2)w(1,3)\,\mathrm{d}2\,\mathrm{d}3 \\ &+ \frac{\rho^3}{4}\iiint\big[g_0^{(4)}(1,2,3,4) - g_0^{(2)}(1,2)g_0^{(2)}(3,4)\big] \\ &\qquad\times w(1,2)w(3,4)\,\mathrm{d}2\,\mathrm{d}3\,\mathrm{d}4\Bigg) \\ &- \tfrac{1}{4}S_0(0)\left(\frac{\partial}{\partial\rho}\left(\rho^2\int g_0(1,2)w(1,2)\,\mathrm{d}2\right)^2\right)\end{aligned} \tag{5.2.15}$$

where $S_0(k)$ is the structure factor of the reference system.

We see from (5.2.15) that a calculation of the second-order term requires a knowledge of the three- and four-particle distribution functions of the reference system. The situation is even more complicated for higher-order terms, since the calculation of F_n requires the distribution functions of all orders up to and including $2n$. By the same rule, calculation of the first-order term requires only the pair distribution function of the reference system. If ε defines the energy scale of the perturbation, truncation at first order is likely to be justified whenever $\beta\varepsilon \ll 1$. The fact that second- and higher-order terms are determined by fluctuations in the total perturbation energy suggests that they should be small, relative to F_1, whenever the perturbing potential is a very smoothly varying function of particle separation. Schemes that simplify the calculation of F_2 have been devised, but the high-temperature expansion remains easiest to apply in situations where terms beyond first order are negligible. The question of whether or not a first-order treatment is adequate depends on the thermodynamic state, the form of the potential $v(1,2)$, and the manner in which $v(1,2)$ is divided into a reference-system potential and a perturbation.

If the reference system is the hard-sphere fluid and the perturbation potential $w(1,2)$ is very long ranged, the high-temperature expansion limited to first order reduces to the van der Waals equation (5.1.2). It is necessary only that the range of $w(1,2)$ be large compared with the range of interparticle separations over which $g_0(1,2)$ is significantly different from its asymptotic value. Then, to a good approximation:

$$\frac{\beta F_1}{N} \approx \frac{\beta\rho}{2}\int w(\mathbf{r})\,\mathrm{d}\mathbf{r} = -\beta\rho a \tag{5.2.16}$$

where a is positive when the perturbing potential is attractive. On differentiating with respect to density we recover (5.1.2):

$$\frac{\beta P}{\rho} = \rho\frac{\partial}{\partial\rho}\left(\frac{\beta F_0}{N} + \frac{\beta F_1}{N}\right) = \frac{\beta P_0}{\rho} - \beta\rho a \tag{5.2.17}$$

Another important feature of the high-temperature expansion is the fact that the first-order approximation yields a rigorous upper bound on the free energy of the system of interest irrespective of the choice of reference system. This result is a further consequence of the Gibbs–Bogoliubov inequalities discussed in Appendix B in connection with the density-functional theory of Section 3.4. Consider two integrable, non-negative but otherwise arbitrary configuration-space functions $A(\mathbf{r}^N)$ and $B(\mathbf{r}^N)$, defined such that[7]

$$\int A\left(\mathbf{r}^N\right)\mathrm{d}\mathbf{r}^N = \int B\left(\mathbf{r}^N\right)\mathrm{d}\mathbf{r}^N \tag{5.2.18}$$

The argument in Appendix B shows that the two functions satisfy the inequality

$$\int A\left(\mathbf{r}^N\right)\ln A\left(\mathbf{r}^N\right)\mathrm{d}\mathbf{r}^N \geqslant \int A\left(\mathbf{r}^N\right)\ln B\left(\mathbf{r}^N\right)\mathrm{d}\mathbf{r}^N \tag{5.2.19}$$

We now make two particular choices for A and B. First, let

$$\begin{aligned} A(\mathbf{r}^N) &= \exp\bigl(\beta\bigl[F_0 - V_N(0)\bigr]\bigr) \\ B(\mathbf{r}^N) &= \exp\bigl(\beta\bigl[F_0 - V_N(1)\bigr]\bigr) \end{aligned} \tag{5.2.20}$$

It follows from (5.2.19) that

$$F \leqslant F_0 + \bigl[\bigl\langle V_N(1)\bigr\rangle_0 - \bigl\langle V_N(0)\bigr\rangle_0\bigr] = F_0 + \langle W_N\rangle_0 \tag{5.2.21}$$

This is precisely the inequality announced earlier. If we interchange the definitions of A and B, i.e. if we set

$$\begin{aligned} A(\mathbf{r}^N) &= \exp\bigl(\beta\bigl[F_0 - V_N(1)\bigr]\bigr) \\ B(\mathbf{r}^N) &= \exp\bigl(\beta\bigl[F_0 - V_N(0)\bigr]\bigr) \end{aligned} \tag{5.2.22}$$

then we find from (5.2.19) that

$$F \geqslant F_0 + \langle W_N\rangle_1 \tag{5.2.23}$$

where the average of the perturbation energy is now taken over the ensemble of the system of interest. This result is less useful than (5.2.21), because the properties of the system of interest are in general unknown. With the assumption of pairwise additivity, (5.2.21) and (5.2.23) may be combined in the form

$$\frac{\beta F_0}{N} + \frac{\beta\rho}{2}\int g(\mathbf{r})w(\mathbf{r})\,\mathrm{d}\mathbf{r} \leqslant \frac{\beta F}{N} \leqslant \frac{\beta F_0}{N} + \frac{\beta\rho}{2}\int g_0(\mathbf{r})w(\mathbf{r})\,\mathrm{d}\mathbf{r} \tag{5.2.24}$$

The second of the inequalities (5.2.24) can be used as the basis for a variational approach to the calculation of thermodynamic properties.[8] The variational procedure consists in choosing a reference-system potential that depends on one or more parameters and then of minimising the last term on the right-hand side of (5.2.24) with respect to those parameters. As we shall see in the next section, the method has been applied with particular success[9] to systems of particles interacting through an inverse-power or "soft-sphere" potential of the form

$$v(r) = \varepsilon(\sigma/r)^n \tag{5.2.25}$$

In these calculations the reference system is taken to be a fluid of hard spheres and the hard-sphere diameter is treated as the single variational parameter. Still better results are obtained if a correction is made for the fact that the configuration space accessible to the hard-sphere and soft-sphere fluids is different for the two systems. The effect of this correction is to add to the right-hand side of (5.2.14) a term[10] involving a ratio of configuration integrals:

$$\frac{\beta\Delta F}{N} = \frac{1}{N}\ln\frac{\int_{\Omega_d}\exp[-\beta V_N(\mathbf{r}^N)]\,\mathrm{d}\mathbf{r}^N}{\int_{\Omega}\exp[-\beta V_N(\mathbf{r}^N)]\,\mathrm{d}\mathbf{r}^N} \tag{5.2.26}$$

where $V_N(\mathbf{r}^N)$ is the total potential energy of the system of interest (the soft-sphere fluid), Ω represents the full configuration space and Ω_d represents that part of configuration space

in which there is no overlap between hard spheres of diameter d. Since Ω_d is smaller than Ω, the correction is always negative, thereby lowering the upper bound on the free energy provided by the inequality (5.2.21). The correction term can be evaluated numerically by a Monte Carlo method,[10(b)] and an approximate but accurate expression for the term has been derived[9] that involves only the pair distribution function of the hard-sphere fluid.

5.3 SOFT-CORE REFERENCE SYSTEMS

Perturbation theories are useful only if they relate the properties of the system of interest to those of a well understood reference system. Hard spheres are an obvious choice of reference system, for the reasons discussed in Section 5.1. On the other hand, realistic intermolecular potentials do not have an infinitely steep repulsive core, and there is no natural separation into a hard-sphere part and a weak perturbation. Instead, an arbitrary division of the potential is made, as in (5.2.1), and the properties of the reference system, with potential $v_0(r)$, are then usually related to those of hard spheres in a manner independent of the way in which the perturbation is treated. In this section we discuss how the relation between the reference system and the system of hard spheres can be established, postponing the question of how best to separate the potential until Section 5.4. We describe in detail only the "blip-function" method of Andersen, Weeks and Chandler,[11] but we also show how results obtained earlier by Rowlinson[12] and by Barker and Henderson[13] can be recovered from the same analysis. In each case the free energy of the reference system is equated to that of a hard-sphere fluid at the same temperature and density. The hard-sphere diameter is, in general, a functional of $v_0(r)$ and a function of ρ and T, and the various methods of treating the reference system differ from each other primarily in the prescription used to determine d.

If the reference-system potential is harshly repulsive but continuous, the Boltzmann factor $e_0(r) = \exp[-\beta v_0(r)]$ typically has the appearance shown in Figure 5.2 and is not very different from the Boltzmann factor $e_d(r)$ of a hard-sphere potential. Thus, for a well chosen value of d, the function

$$\Delta e(r) = e_0(r) - e_d(r) \tag{5.3.1}$$

is effectively non-zero only over a small range of r which we denote by ξd. The behaviour of $\Delta e(r)$ as a function of r is sketched in Figure 5.2; the significance of the name "blip function" given to it is obvious from the figure.

When ξ is small it is natural to seek an expansion of the properties of the reference system about those of hard spheres in powers of ξ. Such a series can be derived by making a functional Taylor expansion of the reduced free-energy density $\phi = -\beta F^{\text{ex}}/V$ in powers of $\Delta e(r)$, i.e.

$$\phi = \phi_d + \int \left.\frac{\delta\phi}{\delta e(\mathbf{r})}\right|_{e=e_d} \Delta e(\mathbf{r})\,\mathrm{d}\mathbf{r} + \tfrac{1}{2}\iint \left.\frac{\delta^2\phi}{\delta e(\mathbf{r})\delta e(\mathbf{r}')}\right|_{e=e_d} \mathrm{d}\mathbf{r}\,\mathrm{d}\mathbf{r}' + \cdots \tag{5.3.2}$$

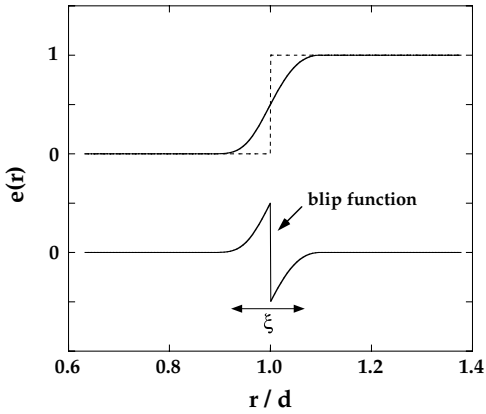

FIG. 5.2. The blip function. The upper part of the figure shows the Boltzmann factors $e_0(r)$ and $e_d(r)$ for soft-core (full curve) and hard-sphere (dashes) potentials, respectively; the lower part shows the blip function, $\Delta e(r) = e_0(r) - e_d(r)$.

where ϕ_d is the free-energy density of the hard-sphere fluid. We know from (2.5.23) and (3.4.8) that the functional derivative of ϕ with respect to $e(\mathbf{r})$ is

$$\frac{\delta\phi}{\delta e(\mathbf{r})} = \tfrac{1}{2}\rho^2 y(\mathbf{r}) \tag{5.3.3}$$

Equation (5.3.2) can therefore be rewritten as

$$\phi = \phi_d + \tfrac{1}{2}\rho^2 \int y_d(\mathbf{r})\,\Delta e(\mathbf{r})\,\mathrm{d}\mathbf{r} + \cdots \tag{5.3.4}$$

The expression for the second-order term involves the three- and four-particle distribution functions of the hard-sphere system, but terms beyond first order are not needed for steep potentials.

Since the range of $\Delta e(r)$ is ξd, the first-order term in the expansion (5.3.2) is of order ξ. A natural choice of d is one that causes the first-order term to vanish; d is then determined by the implicit relation

$$\int y_d(r)\,\Delta e(r)\,\mathrm{d}\mathbf{r} = 0 \tag{5.3.5}$$

With this choice of d, the second-order term in (5.3.2), which would normally be of order ξ^2, becomes of order ξ^4. Thus the free-energy density of the reference system is related to that of the hard-sphere fluid by

$$\phi_0 = \phi_d + \mathcal{O}(\xi^4) \tag{5.3.6}$$

where d is defined by (5.3.5).

Equation (5.3.5) represents only one of many possible prescriptions for calculating the diameter of the "equivalent" hard spheres. Because $\Delta e(r)$ is non-zero only in a narrow range of r, the factor $r^2 y_d(r)$ in (5.3.5) can be expanded in a Taylor series about $r = d$ in the form

$$r^2 y_d(r) = \sigma_0 + \sigma_1\left(\frac{r}{d} - 1\right) + \sigma_2\left(\frac{r}{d} - 1\right)^2 + \cdots \tag{5.3.7}$$

with

$$\frac{\sigma_m}{d^m} = \frac{d^m}{dr^m} r^2 y_d(r)\bigg|_{r=d} \tag{5.3.8}$$

Substitution of the expansion (5.3.7) in (5.3.5) gives

$$\sum_{m=0}^{\infty} \frac{\sigma_m}{m!} I_m = 0 \tag{5.3.9}$$

where

$$\begin{aligned} I_m &= \int_0^\infty \left(\frac{r}{d} - 1\right)^m \Delta e(r)\, \mathrm{d}(r/d) \\ &= -\frac{1}{m+1}\int_0^\infty \left(\frac{r}{d} - 1\right)^{m+1} \frac{\mathrm{d}}{\mathrm{d}r} \exp\bigl[-\beta v_0(r)\bigr]\, \mathrm{d}r \end{aligned} \tag{5.3.10}$$

If $v_0(r)$ varies rapidly with r, the derivative in (5.3.10) is approximately a δ-function at $r = d$ and the series (5.3.9) is rapidly convergent. If only the first term is retained, then $I_0 = 0$, and a straightforward integration shows that

$$d = \int_0^\infty \bigl(1 - \exp\bigl[-\beta v_0(r)\bigr]\bigr)\, \mathrm{d}r \tag{5.3.11}$$

This expression is identical to one derived in a different way by Barker and Henderson.[13] In the case when $v_0(r)$ is a soft-sphere potential of the form (5.2.25), the integral in (5.3.11) can be evaluated explicitly in terms of the Γ-function to give

$$d = \sigma(\varepsilon/k_\mathrm{B}T)^{1/n}\Gamma\left(\frac{n-1}{n}\right) = \sigma(\varepsilon/k_\mathrm{B}T)^{1/n}(1 + \gamma/n) + \mathcal{O}\bigl(1/n^2\bigr) \tag{5.3.12}$$

where $\gamma = 0.5772\ldots$ is Euler's constant. On discarding terms of order $1/n^2$ we recover an expression due to Rowlinson.[12] Rowlinson's calculation is based on an expansion of the free energy in powers of the inverse steepness parameter $\lambda = 1/n$ about $\lambda = 0$ (hard spheres); the work of Barker and Henderson may be regarded as a generalisation of Rowlinson's method to a repulsive potential of arbitrary form.

The main difference between (5.3.5) and (5.3.11) lies in the fact that the former yields a hard-sphere diameter that is a function of both density and temperature, whereas the

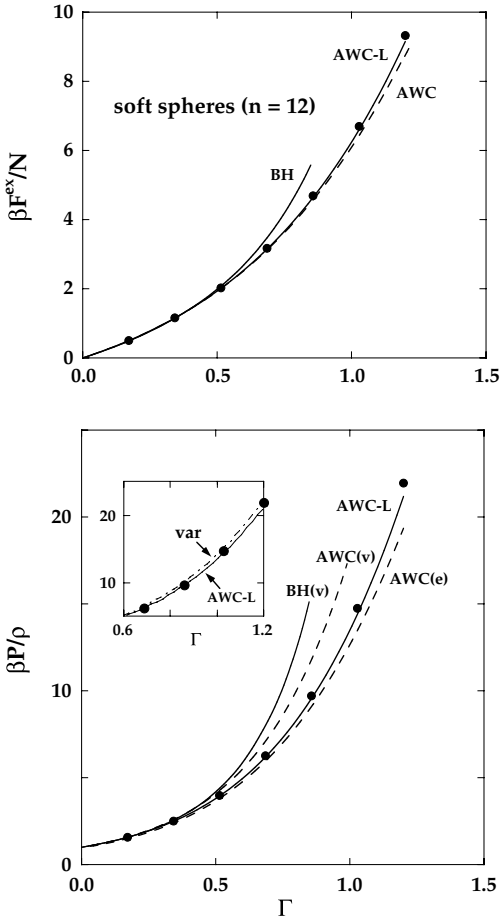

FIG. 5.3. Thermodynamic properties of the r^{-12} fluid.[9,11,13,15] The points are Monte Carlo results[14] and the curves show the predictions of perturbation theory: BH, method of Barker and Henderson, based on (5.3.11); AWC and AWC-L, method of Andersen, Weeks and Chandler, based on (5.3.5) and (5.3.16), respectively. Pressures are calculated from either the virial, (v), or energy, (e), routes, which yield identical results when (5.3.16) is used. The curve labelled "var" in the inset shows the results of a variational calculation[9] in which the correction represented by (5.2.26) is included.

Barker–Henderson diameter is dependent only on temperature. The greater flexibility provided by the use of (5.3.5) ensures that the predictions of the Andersen–Weeks–Chandler approach are, in general, superior to those of the Barker–Henderson theory. The agreement with the results of computer simulations is illustrated for the case of the potential (5.2.25) with $n = 12$ (the r^{-12} fluid) in Figure 5.3. The differences between the results of the two theories becomes smaller as the potential $v_0(r)$ becomes steeper. For inverse-power potentials of this type the excess thermodynamic properties have simple scaling properties, and quantities such as those plotted in the figure are determined by the single, dimensionless

parameter Γ defined as

$$\Gamma = \rho\sigma^3\left(\frac{\varepsilon}{k_{\mathrm{B}}T}\right)^{3/n} \tag{5.3.13}$$

The Andersen–Weeks–Chandler theory also yields a very simple expression for the pair distribution function of the reference system. It follows from (5.3.3) and (5.3.4) that

$$y_0(r) = y_d(r) + \text{higher-order terms} \tag{5.3.14}$$

where the higher-order terms are of order ξ^2 or smaller if d is chosen to satisfy (5.3.5). Thus

$$g_0(r) = \exp\bigl[-\beta v_0(r)\bigr] y_0(r) \approx \exp\bigl[-\beta v_0(r)\bigr] y_d(r) \tag{5.3.15}$$

This expression for the reference-system pair distribution function can now be used, via (5.2.14), to compute the correction to the free energy that results from a perturbing potential $w(r)$. It also allows us to rewrite (5.3.5) in terms of the $k \to 0$ limits of the reference-system and hard-sphere structure factors in the form $S_0(0) = S_d(0)$. Use of the hard-sphere diameter defined by (5.3.5) therefore has the effect of setting the compressibility of the reference system equal to that of the underlying hard-sphere fluid. Equation (5.3.15) is expected to be less accurate than the expression for the free energy, (5.3.6), because the neglected terms are now of order ξ^2 rather than ξ^4. This is borne out by calculations made for the r^{-12}-fluid; the approximate $g_0(r)$ is in only moderate agreement with the results of simulations[14] whereas the agreement obtained for the free energy is very good, as illustrated in Figure 5.3. The situation improves markedly when a much steeper reference potential is involved.

Although the blip-function method works satisfactorily so far as the calculation of thermodynamic properties is concerned, it is clear from Figure 5.3 that there is scope for improvement at large values of Γ, i.e. at high densities or low temperatures. There is also a lack of internal consistency in the theory: pressures calculated from the virial equation (2.5.22) via (5.3.15) differ significantly from those obtained by numerical differentiation of the free energy. The results derived from the free energy are the more reliable, but they are also more troublesome to compute. Equivalence of the two routes to the equation of state is guaranteed, however, if the hard-sphere diameter is calculated, not from (5.3.5), but from the relation[15]

$$\int \frac{\partial y_d(r)}{\partial d}\,\Delta e(\mathbf{r})\,\mathrm{d}\mathbf{r} = 0 \tag{5.3.16}$$

Equation (5.3.16) is derived by requiring that the free energy of the system of interest be a minimum with respect to variations in the hard-sphere function $y_d(r)$. As Figure 5.3 shows, the results obtained for the pressure of the r^{-12}-fluid are thereby much improved.

The blip-function expansion was designed specifically to treat the case of strongly repulsive potentials. This is the case for the Lennard-Jones fluid, which we discuss in the next section. In the repulsive region the Lennard-Jones potential varies much more rapidly than r^{-12}, and the accuracy of the blip-function method in such circumstances could

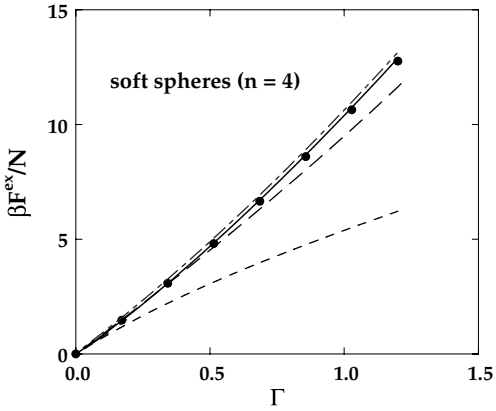

FIG. 5.4. Thermodynamic properties of the r^{-4} fluid. The points are Monte Carlo results and the curves show the predictions of different theories: blip-function method based on (5.3.5) (short dashes) or (5.3.16) (long dashes), and variational theory based on a hard-sphere reference system with (full curve) or without (chain curve) the correction represented by (5.2.26). After Ben-Amotz and Stell.[9]

scarcely be improved upon. The method is less satisfactory for the softer repulsions relevant to liquid metals, because truncation of the expansion (5.3.2) after the first-order term is no longer justified. By contrast, though we see from Figure 5.3 that the hard-sphere variational approach described in Section 5.2 is comparable in accuracy with blip-function theory for $n = 12$, it also retains its accuracy even for $n = 4$ while the first-order blip-function method does not. This is clear from the results shown in Figure 5.4. We also see that within blip-function theory the two prescriptions for the hard-sphere diameter, (5.3.5) and (5.3.16), give rise to significantly larger differences in free energy as the potential is softened. The correction (5.2.26) to the variational calculation is small but not negligible.

5.4 AN EXAMPLE: THE LENNARD-JONES FLUID

The λ-expansion described in Section 5.2 is suitable for treating perturbations that vary slowly in space, while the blip-function expansion and related methods of Section 5.3 provide a good description of reference systems for which the potential is rapidly varying but localised. In this section we show how the two approaches can be combined in a case where the pair potential has both a steep but continuous, repulsive part and a weak, longer ranged attraction. The example we choose is that of the Lennard-Jones fluid, a system for which sufficient data are available from computer simulations to allow a complete test to be made of different perturbation schemes.[16]

At first sight it might appear that the complications due to softness of the core would make it more difficult to obtain satisfactory results by perturbation theory than in situations where the potential consists of a hard-sphere interaction and a tail. This is not necessarily true, however, because there is now the extra flexibility provided by the arbitrary separation of the potential into a reference part, $v_0(r)$, and a perturbation, $w(r)$. A judicious choice of separation can significantly enhance the rate of convergence of the resulting perturbation

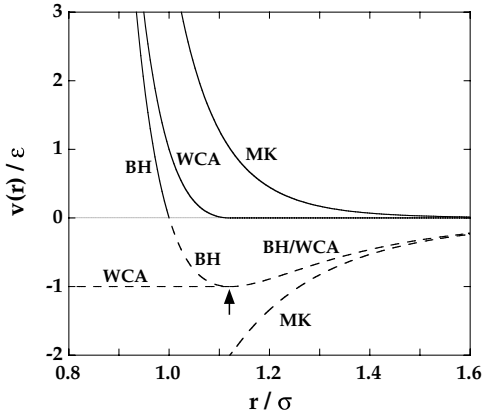

FIG. 5.5. Three separations of the Lennard-Jones potential that have been used in perturbation-theory calculations: MK, by McQuarrie and Katz:[17] BH, by Barker and Henderson;[13] WCA, by Weeks, Chandler and Andersen.[19] Full curves: the reference-system potential; dashes: the perturbation. The arrow marks the position of the minimum in the full pair potential; at larger values of r the Barker–Henderson and WCA choices of perturbation are the same.

series. A number of separations have been proposed for the Lennard-Jones potential, the best known of which are the three illustrated in Figure 5.5.

In the method of McQuarrie and Katz[17] the r^{-12} term is chosen as the reference-system potential and the r^{-6} term is treated as a perturbation. Given a scheme in which the properties of the reference system are calculated accurately, the method works well at temperatures above $T^* \approx 3$. At lower temperatures, however, the results are much less satisfactory. This is understandable, since the reference-system potential is considerably softer than the full potential in the region close to the minimum in $v(r)$. In the separation used by Barker and Henderson[13] the reference system is defined by that part of the full potential which is positive ($r < \sigma$) and the perturbation consists of the part that is negative ($r > \sigma$). The reference-system properties are then related to those of hard spheres of diameter d given by (5.3.11). In contrast to the case of the r^{-12} potential (see Figure 5.3), this treatment of the reference system yields very accurate results. The corrections due to the perturbation are handled in the framework of the λ-expansion; the first-order term is calculated from (5.2.14), with $g_0(r)$ taken to be the pair distribution function of the equivalent hard-sphere fluid. At $T^* = 0.72$ and $\rho^* = 0.85$, which is close to the triple point of the Lennard-Jones fluid, the results are $\beta F_0/N = 3.37$ and $\beta F_1/N = -7.79$. Thus the sum of the two leading terms is equal to -4.42, whereas the resulted obtained for the total excess free energy from Monte Carlo calculations[16] is $\beta F/N = -4.87$. The sum of all higher-order terms in the λ-expansion is therefore far from negligible; detailed calculations show that the second-order term accounts for most of the remainder.[16(a)] The origin of the large second-order term lies in the way in which the potential is separated. As Figure 5.5 reveals, the effect of dividing $v(r)$ at $r = \sigma$ is to include in the perturbation the rapidly varying part of the potential between $r = \sigma$ and the minimum at $r = r_m \approx 1.122\sigma$. Since the pair distribution function has its maximum value in the same range of r, fluctuations in the total perturbation energy W_N, and hence the numerical values of F_2, are large.

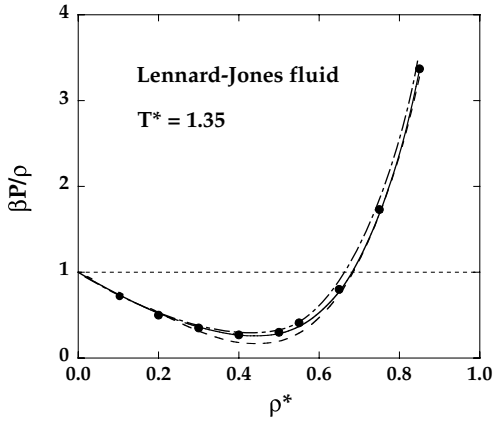

FIG. 5.6. Equation of state of the Lennard-Jones fluid along the isotherm $T^* = 1.35$. The points are Monte Carlo results and the curves show the predictions of perturbation theory. Dashes: WCA theory; chain curve: first-order Barker–Henderson theory; full curve: second-order Barker–Henderson theory. After Barker and Henderson.[18]

The work of Barker and Henderson is a landmark in the development of liquid-state theory, since it demonstrated for the first time that thermodynamic perturbation theory is capable of yielding quantitatively reliable results even for states close to the triple point of the system of interest. A drawback to their method is the fact that its successful implementation requires a careful evaluation of the second-order term in the λ-expansion. The calculation of F_2 from (5.2.15) requires further approximations to be made, and although the hard-sphere data that allow such a calculation are available in analytical form[18] the theory is inevitably more awkward to handle than is the case when a first-order treatment is adequate. Nonetheless, as Figure 5.6 illustrates, the calculated equation of state is in excellent agreement with the results of simulations.

The problem of the second-order term can be overcome by dividing the potential in the manner of Weeks, Chandler and Andersen,[19] usually called the WCA separation. In this method, the potential is split at $r = r_m$ into its purely repulsive ($r < r_m$) and purely attractive ($r > r_m$) parts; the former defines the reference system and the latter constitutes the perturbation. To avoid a discontinuity at $r = r_m$, $w(r)$ is set equal to $-\varepsilon$ for $r < r_m$ and $v_0(r)$ is shifted upwards by a compensating amount. Compared with the Barker–Henderson separation, the perturbation now varies more slowly over the range of r corresponding to the first peak in $g(r)$, and the perturbation series is therefore more rapidly convergent. For example, at $T^* = 0.72$, $\rho^* = 0.85$, the reference-system free energy is $\beta F_0/N = 4.49$ and the first-order correction in the λ-expansion is -9.33; the sum of the two terms is -4.84, which differs by less than 1% from the Monte Carlo result for the full potential.[16(b)] Agreement of the same order is found throughout the high-density region and the perturbation series may confidently be truncated after the first-order term. The difficulties associated with the calculation of the second- and higher-order terms are thereby avoided. At high densities, on the other hand, the hard-sphere diameter calculated for the WCA separation may correspond to a packing fraction lying in the metastable region beyond the fluid–solid transition. This limits the range of applicability of the theory at supercritical temperatures.[20]

In the calculations summarised above, and in most of those based on the WCA separation, the free energy of the reference system is related to that of hard spheres through (5.3.5) and (5.3.6). At high densities, the error (of order ξ^4) thereby introduced is very small. Under the same conditions, use of the approximate relation (5.3.15) to calculate the first-order correction from (5.2.14) also involves only a very small error. Some results for the Lennard-Jones fluid along a near-critical isotherm are shown in Figure 5.6. The general level of agreement with the results of computer simulations is good and at high densities is comparable with that achieved by the Barker–Henderson method taken to second order. At low densities the attractive forces play an important role in determining the structure and the key assumption of a first-order theory, namely that $g(r) \approx g_0(r)$, is no longer valid. New methods are then required, as we discuss in detail in the next section.

5.5 TREATMENT OF ATTRACTIVE FORCES

Situations in which the influence of the attractive forces on the structure cannot be ignored may be treated by methods similar to those used when the perturbation is both weak and very long ranged relative to the reference-system potential. In such cases the natural expansion parameter is the inverse range rather than the strength of the perturbation; this leads to the so-called γ-expansion,[21] the nature of which differs significantly from that of the λ-expansion described in Section 5.2. The early work on the γ-expansion was motivated by the fact that an exact solution can be found for the one-dimensional model of hard rods of length d that attract each other via the potential

$$w_\gamma(x) = -a\gamma \exp(-\gamma x), \quad a\gamma > 0 \tag{5.5.1}$$

where γ is an inverse-range parameter; the integral of $w_\gamma(x)$ over all one-dimensional space is independent of γ and equal to $-a$. Kac, Uhlenbeck and Hemmer[22] have shown that in the limit $\gamma \to 0$, taken *after* the thermodynamic limit, the pressure is given by the one-dimensional van der Waals equation, i.e.

$$\lim_{\gamma \to 0} \frac{\beta P}{\rho} = \frac{1}{1-\rho d} - \beta\rho a \tag{5.5.2}$$

where the first term on the right-hand side represents the exact equation of state of the hard-rod reference system. This result was later extended to three dimensions and it was proved rigorously that in the limit where the perturbation is both infinitesimally strong and infinitely long ranged, the equation of state is given exactly by the generalised van der Waals equation (5.1.2).

The γ-expansion is obtained by considering perturbations of the general form

$$w_\gamma(r) = -\gamma^3 f(\gamma r) \tag{5.5.3}$$

and expanding the properties of the system of interest in powers of γ. If R is the range of the reference-system potential (e.g. the hard-sphere diameter), the dimensionless parameter of the expansion is $\delta = (\gamma R)^3$; δ is roughly the ratio of the reference-system interaction

volume (e.g. the volume of a hard sphere) to the total interaction volume. In most simple liquids the attractive forces are not truly long ranged in the sense of (5.5.3), but many of the results of the γ-expansion can usefully be carried over to such systems by setting $\gamma = 1$. However, rather than following the original derivation of the γ-expansion, we describe instead the closely related but simpler method of Andersen and Chandler.[23] In doing so, we make use of the diagrammatic definitions and lemmas of Section 3.7. We assume throughout that the pair potential has the general form given by (5.1.3).

We first require the diagrammatic expansion of the excess Helmholtz free energy. This can be derived from the corresponding expansion of the single-particle direct correlation function given by (3.8.6), taken for the case of zero external field. By comparison of (3.8.6) with the definition of $c^{(1)}(\mathbf{r})$ in (3.5.1) it can be deduced that the reduced free-energy density $\phi = -\beta F^{\text{ex}}/V$ introduced in Section 5.3 is expressible diagrammatically as

$V\phi =$ [all irreducible diagrams consisting of two or more black ρ-circles and f-bonds]

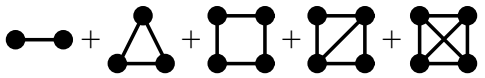

(5.5.4)

If (5.5.4) is inserted in (3.5.1), a simple application of Lemma 2 leads back to (3.8.6).

The separation of the pair potential in (5.1.3) means that the Mayer function $f(1,2)$ can be factorised as

$$f(1,2) = f_0(1,2) + \big[1 + f_0(1,2)\big]\big(\exp\big[\Psi(1,2)\big] - 1\big) \tag{5.5.5}$$

where $f_0(1,2)$ is the Mayer function of the reference system and

$$\Psi(1,2) = -\beta w(1,2) \tag{5.5.6}$$

Since the perturbation is weak, the exponential term in (5.5.5) can be expanded to give

$$f(1,2) = f_0(1,2) + \big[1 + f_0(1,2)\big]\sum_{n=1}^{\infty} \frac{[\Psi(1,2)]^n}{n!} \tag{5.5.7}$$

The form of (5.5.7) suggests the introduction of two different types of bond: short-range f_0-bonds and long-range Ψ-bonds. The presence of two types of bond transforms the simple diagrams in (5.5.4) into composite diagrams in which two circles are linked by at most one f_0-bond but an arbitrary number of Ψ-bonds. We recall from Section 3.7 that if two circles in a diagram are linked by n bonds of a given species, the symmetry number of the diagram is increased, and its value decreased, by a factor $n!$; this takes care of the factors $1/n!$ in (5.5.7). The complete expansion of a in terms of composite diagrams is

$V\phi =$ [all irreducible diagrams consisting of two or more black ρ-circles, f_0-bonds and Ψ-bonds, where each pair of circles is linked by any number of Ψ-bonds but at most one f_0-bond] (5.5.8)

The corresponding expansion of the pair distribution function can be obtained from (3.4.8). Written in the notation of the present section the latter becomes

$$\rho^2 g(1,2) = 2V \frac{\delta \phi}{\delta \Psi(1,2)} \tag{5.5.9}$$

and the diagrammatic prescription for $g(1,2)$ follows immediately from application of Lemma 3.

The sum of all diagrams in (5.5.8) in which only f_0-bonds appear yields the free-energy density ϕ_0 of the reference system. The f_0-bonds in the other diagrams can be replaced in favour of h_0-bonds by a process of topological reduction based on Lemma 5. This leads to the elimination of diagrams containing "reference articulation pairs", which are pairs of circles linked by one or more independent paths consisting exclusively of black circles linked by reference-system bonds.[24] Of the diagrams that remain after the topological reduction there are two of order ρ^2 that contain only a single Ψ-bond. The sum of the two is written as

$V\phi_{\mathrm{HTA}} =$ 

$$= \tfrac{1}{2}\rho^2 \iint \left[\Psi(1,2) + h_0(1,2)\Psi(1,2)\right] \mathrm{d}1\,\mathrm{d}2$$

$$= -\frac{V\beta\rho^2}{2} \int g_0(\mathbf{r}) w(\mathbf{r})\, \mathrm{d}\mathbf{r} \tag{5.5.10}$$

where a broken line represents an h_0-bond, a solid line represents a Ψ-bond and HTA stands for "high-temperature approximation". Comparison of (5.5.10) with (5.2.14) shows that the HTA is equivalent to truncation of the λ-expansion after the first-order term, with

$$\phi_{\mathrm{HTA}} = -\frac{\beta F_1}{V} \tag{5.5.11}$$

The corresponding approximation to $g(1,2)$ is given by a trivial application of Lemma 3. If $\phi \approx \phi_{\mathrm{HTA}}$ we find from (5.5.10) that

$$\rho^2 g(1,2) \approx 2V \frac{\delta \phi_{\mathrm{HTA}}}{\delta \Psi(1,2)}$$

$$= \rho^2 + \rho^2 h_0(1,2) = \rho^2 g_0(1,2) \tag{5.5.12}$$

in agreement with the results of Section 5.3.

To proceed beyond the HTA it is necessary to sum a larger class of diagrams in the expansion of ϕ. An approximation similar in spirit to the Debye–Hückel theory of ionic fluids is

$$\phi \approx \phi_0 + \phi_{\mathrm{HTA}} + \phi_{\mathrm{R}} \tag{5.5.13}$$

where

$V\phi_{\mathrm{R}} =$ 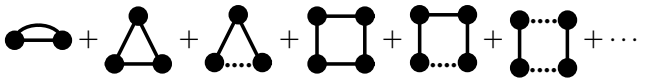 (5.5.14)

is the sum of all simple "ring" diagrams plus the diagram consisting of two black circles linked by two Ψ-bonds; the absence of reference articulation pairs means that none of the ring diagrams in (5.5.14) contains two successive h_0-bonds. The approximation to $g(1,2)$ obtained by applying Lemma 3 is now

$$g(1,2) \approx g_0(1,2) + C(1,2) \tag{5.5.15}$$

where the function $C(1,2)$ is given by

$$\begin{aligned}\rho^2 C(1,2) = [&\text{all chain diagrams consisting of two terminal white}\\ &\rho\text{-circles labelled 1 and 2, black } \rho\text{-circles, } \Psi\text{-bonds}\\ &\text{and } h_0\text{-bonds, where there are never two successive}\\ &h_0\text{-bonds}]\end{aligned} \tag{5.5.16}$$

If the reference system is the ideal gas and if $w(r)$ is the Coulomb potential, then $-k_{\mathrm{B}}TC(1,2)$ is the screened potential $\psi(r)$ of (4.6.25) and (5.5.15) reduces to the linearised Debye–Hückel result (4.6.27). For the systems of interest here, $-k_{\mathrm{B}}TC(1,2)$ is a renormalised potential in which the perturbation is screened by the order imposed on the fluid by the short-range interaction between particles.

The function $C(1,2)$ can be evaluated by Fourier transform techniques similar to those used in the derivation of the Debye–Hückel result. We first group the chain diagrams according to the number of Ψ-bonds they contain. Let $C^{(n)}(1,2)$ be the sum of all chain diagrams with precisely n Ψ-bonds. Then

$$\rho^2 C(1,2) = \rho^2 \sum_{n=1}^{\infty} C^{(n)}(1,2) \tag{5.5.17}$$

where

$\rho^2 C^{(1)}(1,2) =$ 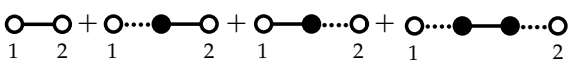 (5.5.18)

and so on. Any diagram that contributes to $C^{(n)}$ contains at most $(n+1)$ h_0-bonds and $C^{(n)}$ consists of 2^{n+1} topologically distinct diagrams.

The sum of all diagrams in $C^{(n)}(1,2)$ may be represented by a single "generalised chain" in which circles are replaced by *hypervertices*. A hypervertex of order n is associated with a function of n coordinates, $\Sigma(1,\ldots,n)$, and is pictured as a large circle surrounded by

n white circles; the latter correspond, as usual, to the coordinates $\mathbf{r}_1, \ldots, \mathbf{r}_n$. For present purposes we need consider only the hypervertex of order two associated with the reference-system function $\Sigma_0(1,2)$ defined as

$$\Sigma_0(1,2) = \rho\delta(1,2) + \rho^2 h_0(1,2)$$
$$= \quad 1 \quad 2 \tag{5.5.19}$$

We can then re-express $C^{(n)}(1,2)$ for $n=1$ and $n=2$ in the form

$$\rho^2 C^{(1)}(1,2) = \iint \Sigma_0(1,3)\Psi(3,4)\Sigma_0(4,2)\,\mathrm{d}3\,\mathrm{d}4 \tag{5.5.20}$$
$$= \quad 1 \quad 2$$

$$\rho^2 C^{(2)}(1,2) = \quad 1 \quad 2 \tag{5.5.21}$$

and $\rho^2 C^{(n)}(1,2)$ for any n is represented by a generalised chain consisting of n Ψ-bonds and $(n+1)$ Σ_0-hypervertices. Each generalised chain corresponds to a convolution integral with a Fourier transform given by

$$\rho^2 \widehat{C}^{(n)}(\mathbf{k}) = \left[\widehat{\Sigma}_0(\mathbf{k})\widehat{\Psi}(\mathbf{k})\right]^n \widehat{\Sigma}_0(\mathbf{k}) \tag{5.5.22}$$

where $\widehat{\Sigma}_0(\mathbf{k})$ is related to the structure factor of the reference system by $\widehat{\Sigma}_0(\mathbf{k}) = \rho S_0(\mathbf{k})$ and $\widehat{\Psi}(\mathbf{k}) = -\beta\widehat{w}(\mathbf{k})$. If $|\widehat{\Sigma}_0(\mathbf{k})\widehat{\Psi}(\mathbf{k})| < 1$, the Fourier transform of the function $C(1,2)$ is obtained as the sum of a geometric series:

$$\rho^2 \widehat{C}(\mathbf{k}) = \sum_{n=1}^{\infty} \rho^2 \widehat{C}^{(n)}(\mathbf{k}) = \frac{[\widehat{\Sigma}_0(\mathbf{k})]^2 \widehat{\Psi}(\mathbf{k})}{1 - \widehat{\Sigma}_0(\mathbf{k})\widehat{\Psi}(\mathbf{k})} = -\frac{\rho^2 [S_0(\mathbf{k})]^2 \beta\widehat{w}(\mathbf{k})}{1 + \rho S_0(\mathbf{k})\beta\widehat{w}(\mathbf{k})} \tag{5.5.23}$$

The derivation of (5.5.23) tends to obscure the basic simplicity of the theory. If (4.1.5), (5.5.15) and (5.5.23) are combined, we find that the structure factor of the system of interest is related to that of the reference fluid by

$$S(\mathbf{k}) = S_0(\mathbf{k}) - \frac{\rho[S_0(\mathbf{k})]^2 \beta\widehat{w}(\mathbf{k})}{1 + \rho S_0(\mathbf{k})\beta\widehat{w}(\mathbf{k})} = \frac{S_0(\mathbf{k})}{1 + \rho S_0(\mathbf{k})\beta\widehat{w}(\mathbf{k})} \tag{5.5.24}$$

On the other hand, we find with the help of (3.6.10) that the exact relation between the two structure factors is given in terms of the corresponding direct correlation functions by

$$S(\mathbf{k}) = \frac{S_0(\mathbf{k})}{1 - \rho[\hat{c}(\mathbf{k}) - \hat{c}_0(\mathbf{k})]S_0(\mathbf{k})} \tag{5.5.25}$$

Use of (5.5.24) is therefore equivalent to replacing the true direct correlation function by the random-phase approximation (RPA) of (3.5.17), i.e.

$$c(r) \approx c_0(r) - \beta w(r) \tag{5.5.26}$$

which is asymptotically correct if the perturbation contains the long-range part of the potential. The Debye–Hückel approximation corresponds to writing $c(r) \approx -\beta w(r)$; (5.5.26) improves on this by building in the exact form of the direct correlation function of the reference system.

The RPA approximation for the free energy is obtained by combining (5.5.10), (5.5.13) and (5.5.14). When functionally differentiated with respect to $\Psi(1,2)$ according to the rule (5.5.12), the total ring-diagram contribution to ϕ yields the function $C(1,2)$. It follows that $V\phi_{\mathrm{R}}$ can be expressed diagrammatically as

$$V\phi_{\mathrm{R}} = \sum_{n=2}^{\infty} R^{(n)} \tag{5.5.27}$$

where $R^{(n)}$ is a generalised ring consisting of Σ_0-hypervertices and Ψ-bonds. A generalised ring can be derived from a generalised chain by inserting a Ψ-bond between the white circles and integrating over the coordinates associated with those circles. Thus

$$\begin{aligned} R^{(n)} &= \frac{\rho^2}{2n} \iint C^{(n-1)}(1,2)\Psi(1,2)\,\mathrm{d}1\,\mathrm{d}2 \\ &= \frac{V\rho^2}{2n} \int C^{(n-1)}(\mathbf{r})\Psi(\mathbf{r})\,\mathrm{d}\mathbf{r} \\ &= \frac{V\rho^2}{2n}(2\pi)^{-3} \int \widehat{C}^{(n-1)}(\mathbf{k})\widehat{\Psi}(\mathbf{k})\,\mathrm{d}\mathbf{k} \end{aligned} \tag{5.5.28}$$

where the factor $1/2n$ comes from the symmetry number of the generalised ring. If we now substitute for $\widehat{C}^{(n-1)}(\mathbf{k})$ from (5.5.22) and assume again that $|\widehat{\Sigma}_0(\mathbf{k})\widehat{\Psi}(\mathbf{k})| < 1$, we find that the contribution to ϕ from the ring diagrams is

$$\begin{aligned} \phi_{\mathrm{R}} &= \left(\frac{1}{2\pi}\right)^3 \int \sum_{n=2}^{\infty} \frac{1}{2n}\left[\widehat{\Sigma}_0(\mathbf{k})\widehat{\Psi}(\mathbf{k})\right]^n \mathrm{d}\mathbf{k} \\ &= -\tfrac{1}{2}(2\pi)^{-3} \int \left(\widehat{\Sigma}_0(\mathbf{k})\widehat{\Psi}(\mathbf{k}) + \ln\left[1 - \widehat{\Sigma}_0(\mathbf{k})\widehat{\Psi}(\mathbf{k})\right]\right) \mathrm{d}\mathbf{k} \end{aligned} \tag{5.5.29}$$

This result is used in the discussion of hierarchical reference theory in Section 5.7.

We saw in Section 4.6 that a defect of the linearised Debye–Hückel approximation is the fact that it yields a pair distribution function that behaves unphysically at small separations. A similar problem arises here. Consider, for simplicity, the case in which the reference system is a fluid of hard spheres of diameter d. In an exact theory, $g(r)$ necessarily vanishes

for $r < d$, but in the approximation represented by (5.5.15) there is no guarantee that this will be so, since in general $C(r)$ will be non-zero in that region. There is, however, some flexibility in the choice of $C(r)$, and this fact can be usefully exploited. Although $C(r)$ is a functional of $w(r)$, it is obvious on physical grounds that the true properties of the fluid must be independent of the choice of perturbation for $r < d$. The unphysical behaviour of the RPA can therefore be eliminated by choosing $w(r)$ for $r < d$ in such a way that

$$C(r) = 0, \quad r < d \tag{5.5.30}$$

Comparison of (5.5.15) with the general rule (5.5.9) shows that this condition is equivalent to requiring the free energy to be stationary with respect to variations in the perturbing potential within the hard core. The RPA together with the condition (5.5.30) is called the "optimised" random-phase approximation or ORPA. The ORPA may also be regarded as a solution to the Ornstein–Zernike relation that satisfies both the closure relation (5.5.26) and the restriction that $g(r) = 0$ for $r < d$. It is therefore similar in spirit to the MSA of Section 4.5, the difference being that the treatment of the hard-sphere system is exact in the ORPA.

The derivation of (5.5.24) did not involve any assumption about the range of the potential $w(r)$. However, as we have seen in Section 3.5, the RPA can also be derived by treating the effects of the perturbation in a mean-field way, an approximation that is likely to work best when the perturbation is both weak and long ranged. In practice the optimised version of the theory gives good results for systems such as the Lennard-Jones fluid.[25] Not surprisingly, however, it is less successful when the attractive well in the potential is both deep and narrow.[26] In that case better results are obtained by replacing $-\beta w(r)$ in (5.5.26) by the corresponding Mayer function; this modification also ensures that $c(r)$ behaves correctly in the low-density limit.

A different method of remedying the unphysical behaviour of the RPA pair distribution function can be developed by extending the analogy with Debye–Hückel theory. If the reference system is the ideal gas, the RPA reduces to

$$g(1, 2) \approx 1 + C(1, 2) \tag{5.5.31}$$

When $w(r)$ is the Coulomb potential, this result is equivalent to the linearised Debye–Hückel approximation (4.6.27). If we add to the right-hand side of (5.5.28) the sum of all diagrams in the exact expansion of $h(1, 2)$ that can be expressed as star products of the diagram $C(1, 2)$ with itself, and then apply Lemma 1, we obtain an improved approximation in the form

$$\begin{aligned} g(1, 2) &\approx \exp C(1, 2) \\ &= 1 + \underset{1\quad 2}{\circ\!\!-\!\!\circ} + \underset{1\quad 2}{\circ\!\!\frown\!\!\circ} + \underset{1\quad 2}{\circ\!\!\rightleftharpoons\!\!\circ} + \cdots \end{aligned} \tag{5.5.32}$$

which is equivalent to the non-linear equation (4.6.26). In the present case a generalisation of the same approach replaces the RPA of (5.5.15) by the approximation

$$g(1, 2) \approx g_0(1, 2) \exp C(1, 2) \tag{5.5.33}$$

This is called the "exponential" or EXP approximation. At low density the renormalised potential behaves as $C(r) \approx \Psi(r) = -\beta w(r)$. In the same limit, $g_0(r) \approx \exp[-\beta v_0(r)]$. Thus, from (5.5.33):

$$\lim_{\rho \to 0} g(1,2) = \exp\bigl[-\beta v_0(r)\bigr] \exp\bigl[-\beta w(r)\bigr] = \exp\bigl[-\beta v(r)\bigr] \tag{5.5.34}$$

The EXP approximation, unlike either the HTA or the ORPA, is therefore exact in the low-density limit. Andersen and Chandler[23] give arguments to show that the contribution from diagrams neglected in the EXP approximation is minimised if the optimised $C(1,2)$ is used in the evaluation of (5.5.33) and the related expression for the free energy.

The ORPA and the EXP approximation with optimised $C(1,2)$ both correspond to a truncation of the diagrammatic expansion of the free energy in terms of ρ-circles, h_0-bonds and Ψ-bonds in which the perturbation inside the hard core is chosen so as to increase the rate of convergence. Each is therefore an approximation within a general theoretical framework called "optimised cluster theory". The optimised cluster expansion is not in any obvious way a systematic expansion in powers of a small parameter, but it has the great advantage of yielding successive approximations that are easy to evaluate if the pair distribution function of the reference system is known. The γ-expansion provides a natural ordering of the perturbation terms in powers of γ^3, but it leads to more complicated expressions for properties of the system of interest. If the perturbation is of the form of (5.5.3), the terms of order γ^3 in the expansion of the free energy consist of the second of the two diagrams in (5.5.10) (the HTA) and the sum of all diagrams in (5.5.14) (the ring diagrams). There is, in addition, a term of zeroth order in γ, given by the first of the two diagrams in (5.5.10), which in this case has the value

$$\frac{V\beta\rho^2\gamma^3}{2} \int f\bigl(\gamma^3 \mathbf{r}\bigr)\, \mathrm{d}\mathbf{r} = V\beta\rho^2 a \tag{5.5.35}$$

where a is the constant introduced in (5.2.16). We see that the effect of the volume integration is to reduce the apparent order of the term from γ^3 to γ^0. As a consequence, the free energy does not reduce to that of the reference system in zeroth order. It yields instead the van der Waals approximation; the latter is therefore exact in the limit $\gamma \to 0$. Through order γ^3, the free energy (with $\gamma = 1$) is the same as in the RPA. On the other hand, the sum of all terms of order γ^3 in the expansion of $g(1,2)$ contains diagrams additional to the chain diagrams included in (5.5.15).[27]

Results obtained by the optimised cluster approach for a potential model consisting of a hard-sphere core plus a Lennard-Jones tail at two different thermodynamic states are compared with the results of Monte Carlo calculations in Figure 5.7. In the lower-density state, the HTA, ORPA and EXP pair distribution functions represent successively improved approximations to the "exact" results. At the higher density, where the perturbation is heavily screened and the renormalised potential is correspondingly weak, the HTA is already very satisfactory. The difference in behaviour between the two states reflects the diminishing role of the attractive forces on the structure of the fluid as the density increases. Similar conclusions have been reached for other model fluids. Overall the results obtained by opti-

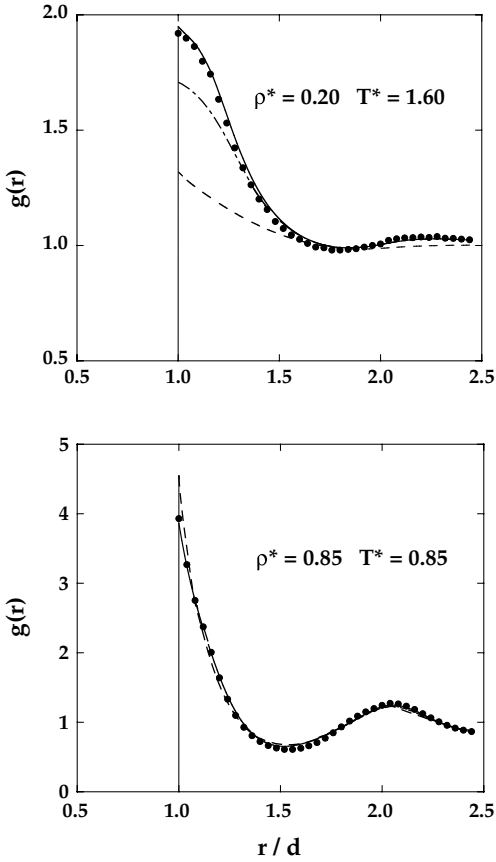

FIG. 5.7. Radial distribution function for a fluid of hard spheres with a Lennard-Jones tail at two different thermodynamic states. The points are Monte Carlo results and the curves show the predictions of perturbation theory. Dashes: HTA; chain curve; ORPA; full curves: EXP. After Stell and Weis.[28]

mised cluster methods are comparable in accuracy with those of conventional perturbation theory taken to second order.

5.6 MEAN-FIELD THEORY OF LIQUID–VAPOUR COEXISTENCE

Coexistence of liquid and vapour arises from a balance between repulsive and attractive intermolecular forces. In the absence of any attractive interactions, there is no liquid–vapour transition, and only one fluid phase appears. Since perturbation theory is based explicitly on a division of the pair potential into repulsive and attractive parts, it is a natural choice for the description of phenomena associated with condensation. The integral-equation approximations described in Chapter 4 provide another possible approach, but for the most part they either lead to spurious solutions or do not converge numerically in the thermody-

namic region of interest.[29] These failings are a consequence of the underlying singularities in thermodynamic properties, in particular the divergence of the isothermal compressibility at the critical point.

For a two-phase system to be in equilibrium, each phase must be at the same pressure (mechanical equilibrium) and temperature (thermal equilibrium). However, the pressure and temperature of a two-phase system are not independent variables, since equality of the chemical potentials or, equivalently, of the molar Gibbs free energies is also required. Thus, at equilibrium between liquid (L) and gas (G) in a one-component system:

$$\mu_{\mathrm{L}}(P,T)=\mu_{\mathrm{G}}(P,T) \tag{5.6.1}$$

If μ_{L} and μ_{G} are known from some approximate theory, (5.6.1) can be solved for P as a function of T to yield the phase-coexistence curve in the pressure–temperature plane. Condensation is a first-order phase transition, since it coincides with discontinuities in the first-order thermodynamic derivatives of the Gibbs free energy. The volume change, ΔV, corresponds to a discontinuity in $(\partial G/\partial P)_T$, while the change in entropy, ΔS, corresponds to a discontinuity in $(\partial G/\partial T)_P$; ΔS is related to the latent heat of the transition by $L = T\Delta S$. Differentiation of the equilibrium condition (5.6.1) with respect to temperature leads to the Clapeyron equation:

$$\frac{\mathrm{d}P}{\mathrm{d}T}=\frac{\Delta S}{\Delta V}=\frac{L}{T\Delta V} \tag{5.6.2}$$

Since V and S both increase on vaporisation, it follows that the slope of the coexistence curve is always positive.

We consider again a system for which the pair potential $v(r)$ consists of a hard-sphere repulsion supplemented by an attractive term, $w(r)$, for $r > d$, where, as usual, d is the hard-sphere diameter. If $w(r)$ is sufficiently long ranged, the free energy may be approximated by the first two terms of the λ-expansion of Section 5.2 or, within the mean-field approximation (5.2.16), by

$$\frac{\beta F}{N}=\frac{\beta F_0}{N}-\beta\rho a \tag{5.6.3}$$

where F_0, the free energy of the hard-sphere reference system, is a function only of the packing fraction η. The equation of state is then given by (5.2.17). We are interested primarily in the calculation of thermodynamic properties in the critical region. Since the critical density ρ_{c} is typically less than half that of the triple point, it is reasonable to approximate the hard-sphere pressure by the Percus–Yevick compressibility equation (4.4.12), which is very accurate at low to moderate densities. Thus

$$\frac{\beta P}{\rho}=\frac{1+\eta+\eta^2}{(1-\eta)^3}-\beta\rho a \tag{5.6.4}$$

Above a critical temperature T_{c}, to be determined below, the pressure isotherms calculated from (5.6.4) are single-valued, increasing functions of ρ, as sketched in Figure 5.8. Below T_{c}, however, so-called van der Waals loops appear, which contain an unphysical section between their maxima and minima where the isothermal compressibility would

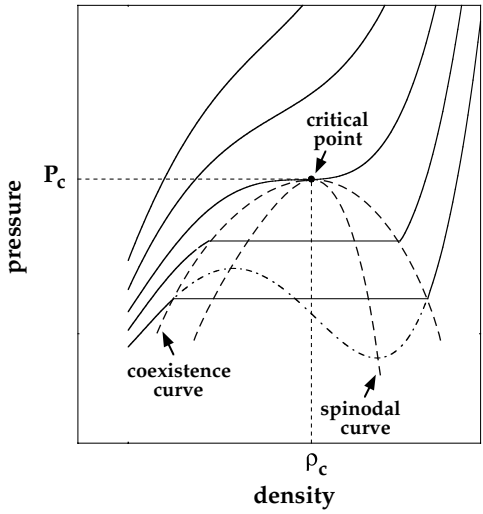

FIG. 5.8. Isotherms of a simple fluid in the pressure–density plane. The chain curve shows a van der Waals loop. Note that the Maxwell construction applies in the pressure–volume, not the pressure–density plane.

be negative, thereby violating one of the conditions necessary for stability of the system against fluctuations (see Appendix A). The unstable states are eliminated by replacing the loops by horizontal portions between points on the isotherm determined via the Maxwell equal-area construction in the P–V plane. The Maxwell construction is a graphical formulation of the requirement for equality of the pressures and chemical potentials of the two phases; it is equivalent[30] to the double-tangent construction on a plot of free energy versus volume, which ensures that F is always a convex function, i.e. that $(\partial^2 F/\partial V^2)_T > 0$. The end-points of the horizontal portions lie on the coexistence curve, while the locus of maxima and minima of the van der Waals loops, which separates the P–ρ plane into stable and unstable regions, forms the *spinodal* curve. States lying between the coexistence and spinodal curves are metastable, but can be reached experimentally if sufficient care is taken to prevent formation of the thermodynamically stable phase. As the temperature increases towards the critical value, the horizontal portion of the isotherm shrinks, eventually reducing to a point of inflection with a horizontal tangent. The critical parameters T_c and ρ_c are therefore determined by the conditions

$$\left(\frac{\partial P}{\partial \rho}\right)_{T=T_c} = 0, \qquad \left(\frac{\partial^2 P}{\partial \rho^2}\right)_{T=T_c} = 0 \tag{5.6.5}$$

The first of these conditions confirms that the compressibility diverges at the critical point; it also diverges everywhere along the spinodal curve, the apex of which coincides with the critical point. The two coexisting phases, liquid and vapour, merge at the critical point, so the transition, which is of first order below T_c, becomes of second order. Second-order transitions are characterised by discontinuities in the second derivatives of the free energy, of which the compressibility is one.

Equations (5.6.4) and (5.6.5) can be solved for the three unknowns: ρ_c, T_c and P_c (the critical pressure). Elimination of T and P leads to a cubic equation in ρ having two unphysical, negative roots and one positive root:

$$\rho_c d^3 \approx 0.245 \tag{5.6.6a}$$

with a corresponding critical temperature given by

$$k_B T_c \approx 0.179 a/d^3 \tag{5.6.6b}$$

and a critical compressibility ratio

$$Z_c = \frac{P_c}{\rho_c k_B T_c} \approx 0.359 \tag{5.6.6c}$$

Both ρ_c and Z_c are independent of the strength of the interparticle attraction, as measured by the value of the quantity a. The theoretical results can be compared with those obtained by molecular-dynamics calculations for a square-well fluid.[31] In this case, $a = \frac{2}{3}\varepsilon\pi d^3(\gamma^3 - 1)$, where γd is the range of the potential and ε is the depth of the square well (see Figure 1.2(a)). The simulations give $\rho_c d^3 \approx 0.34$, $k_B T_c \approx 0.25 a/d^3$ and $Z_c \approx 0.28$, so the agreement with theory is only semi-quantitative. The discrepancies can be ascribed to the use in the theory of the mean-field approximation for the first-order term in the high-temperature expansion and the neglect of higher-order terms. Although the fluctuations corresponding to the higher-order terms are small for liquids at densities close to freezing, they increase rapidly as the density is reduced.

The deficiencies of mean-field theory are also evident in the predictions to which it leads for the behaviour of thermodynamic properties in the immediate vicinity of the critical point. In the approximation represented by (5.6.4) the pressure is an analytic function of ρ and T over a range of packing fraction that extends well beyond the value corresponding to close packing, i.e. $\eta = \pi\sqrt{2}/6 \approx 0.74$. It is therefore legitimate to expand P around P_c in powers of the deviations $\Delta\rho = \rho - \rho_c$ and $\Delta T = T - T_c$. Expansion up to third order gives

$$P = P_c + P_{10}\Delta T + P_{11}\Delta T\,\Delta\rho + P_{03}(\Delta\rho)^3 + \cdots \tag{5.6.7}$$

where the coefficients P_{ij} are

$$P_{ij} = \left(\frac{\partial^{i+j} P}{\partial T^i \partial \rho^j}\right)_{\rho=\rho_c, T=T_c} \tag{5.6.8}$$

Terms in $\Delta\rho$ and $(\Delta\rho)^2$ are zero by virtue of the conditions (5.6.5) and other omitted terms play no role in the derivation that follows. Along the critical isotherm, $\Delta T = 0$, and (5.6.7) simplifies to

$$\Delta P = P - P_c \sim (\Delta\rho)^3, \qquad T = T_c \tag{5.6.9}$$

Thus the critical isotherm is predicted to have an antisymmetric, cubic form. Division of both sides of (5.6.7) by $\Delta\rho$ gives

$$P_{03}(\Delta\rho)^2 = \frac{\Delta P}{\Delta\rho} - P_{10}\frac{\Delta T}{\Delta\rho} - P_{11}\Delta T \tag{5.6.10}$$

On taking the limit $\Delta T \to 0$, we find that

$$\begin{aligned} \frac{\Delta P}{\Delta\rho} &\to \left(\frac{\partial P}{\partial\rho}\right)_{T=T_c} = 0 \\ \frac{\Delta T}{\Delta\rho} &\to \left(\frac{\partial T}{\partial\rho}\right)_P = -\left(\frac{\partial P}{\partial\rho}\right)_{T=T_c} \Bigg/ \left(\frac{\partial P}{\partial T}\right)_{\rho=\rho_c} = 0 \end{aligned} \tag{5.6.11}$$

where the second result follows from the fact that $(\partial P/\partial T)_\rho$ is always positive. Thus (5.6.10) reduces to

$$\Delta\rho = \pm B|\Delta T|^{1/2}, \quad T < T_c \tag{5.6.12}$$

where $B^2 = P_{11}/P_{03} > 0$. The coexistence curve close to the critical point should therefore be symmetrical about $\rho = \rho_c$, i.e. $(\rho_G - \rho_c) = -(\rho_L - \rho_c)$ and $\rho_L + \rho_G = 2\rho_c$. This is a special case of the empirical law of "rectilinear diameters", according to which $\rho_L + \rho_G$ is a linear function of temperature.

Next we consider the behaviour of the isothermal compressibility. From (5.6.7) we see that near the critical point:

$$\left(\frac{\partial P}{\partial\rho}\right)_T \approx P_{11}\Delta T + P_{03}(\Delta\rho)^2 \tag{5.6.13}$$

Along the critical isotherm, where $\Delta\rho = 0$, we find that

$$\chi_T = \frac{1}{\rho}\left(\frac{\partial\rho}{\partial P}\right)_T \approx \frac{1}{P_{11}\rho_c}(\Delta T)^{-1}, \quad T \to T_c^+ \tag{5.6.14a}$$

Along the coexistence curve, (5.6.12) applies. Thus

$$\chi_T \approx \frac{1}{2P_{11}\rho_c}|\Delta T|^{-1}, \quad T \to T_c^- \tag{5.6.14b}$$

Finally, it is easy to show that the specific heat C_V exhibits a finite discontinuity as the critical point is approached along either the critical isochore or the coexistence curve.

Equations (5.6.9), (5.6.12) and (5.6.14) are examples of the *scaling laws* that characterise the behaviour of a fluid close to the critical point, some of which are summarised in Table 5.1. Scaling laws are expressed in terms of certain experimentally measurable *critical exponents* (α, β, γ, etc.), which have the same values for all fluids, irrespective of their chemical nature.[33] This *universality* extends to the behaviour of the Ising model and

TABLE 5.1. *Definitions of the critical scaling laws and numerical values of the exponents*

	Definition	$T - T_c$	$\rho - \rho_c$	Expt[32]	Classical
α	$C_V = A(T - T_c)^{-\alpha}$	>0	0	0.10 ± 0.05	0*
α'	$C_V = A'\lvert T - T_c\rvert^{-\alpha'}$	<0	$\neq 0$		0*
β	$\rho_L - \rho_G = B\lvert T - T_c\rvert^{\beta}$	<0	$\neq 0$	0.32 ± 0.01	$\frac{1}{2}$
γ	$\chi_T = C(T - T_c)^{-\gamma}$	>0	0	1.24 ± 0.1	1
γ'	$\chi_T = C\lvert T - T_c\rvert^{-\gamma'}$	<0	$\neq 0$		1
δ	$\lvert P - P_c\rvert = D\lvert\rho - \rho_c\rvert^{\delta}$	0	$\neq 0$	4.8 ± 0.2	3
ν	$\xi = \xi_0(T - T_c)^{-\nu}$	>0	0	0.63 ± 0.04	$\frac{1}{2}$
ν'	$\xi = \xi_0'\lvert T - T_c\rvert^{-\nu'}$	<0	$\neq 0$		$\frac{1}{2}$

*Finite discontinuity.

other magnetic systems near the paramagnetic–ferromagnetic transition. By comparing the definitions of the scaling laws in Table 5.1 with the results of the mean-field calculations, we can identify the so-called classical values of some of the critical exponents: $\alpha = \alpha' = 0$ (a finite discontinuity), $\beta = \frac{1}{2}$, $\gamma = \gamma' = 1$ and $\delta = 3$. These results differ significantly from the experimental values listed in the table. The classical values are independent of the explicit form of the equation of state. They follow solely from the assumption that the pressure or, equivalently, the free energy is an analytic function of ρ and T close to the critical point and can therefore be expanded in a Taylor series.[34] Analyticity also implies that the classical exponents should be independent of the spatial dimensionality, which is in contradiction both with experimental findings and with exact, theoretical results for the Ising model. The hypothesis of analyticity at the critical point, inherent in mean-field theory, must therefore be rejected. The presence of mathematical singularities in the free energy, reflected in the fact that the true critical exponents are neither integers nor simple, rational numbers, can be traced back to the appearance of large-scale density fluctuations near the critical point. For any finite system, the partition function and free energy are analytic functions of the independent thermodynamic variables. Singularities appear only in the thermodynamic limit, where fluctuations of very long wavelength become possible. Finite systems therefore behave classically, as the results of computer simulations have shown. Extrapolation techniques based on finite-size scaling ideas are needed if non-classical values of the exponents are to be obtained by simulation.[35]

On approaching the critical point, the amplitude of density fluctuations increases and local fluctuations become correlated over increasingly long distances. The compressibility equation (2.6.12) shows that the divergence of the compressibility must be linked to a divergence in the range of the pair correlation function $h(r)$; the range of $h(r)$ is called the *correlation length*, ξ. The behaviour of ξ for $T \approx T_c$ is described by critical exponents ν (along the critical isochore as $T \to T_c^+$) and ν' (along the coexistence curve as $T \to T_c^-$). These exponents are measurable by light and x-ray scattering experiments. Anomalies in the intensity of light scattered from a fluid near its critical point, particularly the phenomenon known as critical opalescence, were first studied theoretically by Ornstein and Zernike as far back as 1914; it was in the course of this work that the direct correlation function

was introduced. Equation (3.5.15) shows that close to the critical point, $\hat{c}(k)$ is of order $1/\rho$ at $k = 0$. Thus the range of $c(r)$ remains finite, which is consistent with the conjecture that $c(r) \to -\beta v(r)$ as $r \to \infty$ (see the discussion following (3.8.7)). If we also assume that $\hat{c}(k)$ has no singularities, it can be expanded in a Taylor series about $k = 0$ in the form

$$\rho\hat{c}(k) = c_0(\rho, T) + c_2(\rho, T)k^2 + \mathcal{O}(k^4) \tag{5.6.15}$$

with

$$\begin{aligned} c_0(\rho, T) &= \rho\hat{c}(0) = 1 - 1/\rho k_B T \chi_T \\ c_2(\rho, T) &= -\tfrac{1}{6}\rho \int c(r) r^2 \, d\mathbf{r} \equiv -R^2 \end{aligned} \tag{5.6.16}$$

The characteristic length R is sometimes called the Debye persistence length. Note that the conjecture regarding the asymptotic behaviour of $c(r)$ means that c_2 and higher-order coefficients in (5.6.16) are strictly defined only for pair potentials $v(r)$ of sufficiently short range.

The key assumption of Ornstein–Zernike theory is that R remains finite at the critical point. Equations (3.6.10) and (5.6.15) then imply that

$$\frac{1}{S(k)} = 1 - \rho\hat{c}(k) \approx 1 - c_0(\rho, T) - c_2(\rho, T)k^2 \tag{5.6.17a}$$

or, from (5.6.16):

$$S(k) = 1 + \rho\hat{h}(k) \approx \frac{R^{-2}}{K^2 + k^2} \tag{5.6.17b}$$

where $K^2 = (1 - c_0)R^{-2} = R^{-2}/\rho k_B T \chi_T$. The asymptotic form of the pair correlation function is obtained by taking the Fourier transform of (5.6.17b):

$$h(r) \sim \frac{1}{4\pi\rho R^2} \frac{\exp(-Kr)}{r}, \quad r \to \infty \tag{5.6.18}$$

The form of this expression makes it natural to identify K with the inverse range of $h(r)$, i.e. with the inverse correlation length:

$$\xi = K^{-1} = R(\rho k_B T \chi_T)^{1/2} \tag{5.6.19}$$

From (5.6.19) and Table 5.1 it is obvious that within the Ornstein–Zernike approximation the critical exponents for ξ and χ_T are related by $\nu = \frac{1}{2}\gamma$. There are indications, however, that the theory is not entirely correct at the critical point. First, it breaks down in two dimensions, where it predicts that $h(r) \sim \ln r$ for large r, which is clearly absurd. Secondly, careful study of plots of $1/S(k)$ versus k^2 shows that the experimental data are not strictly linear, as suggested by (5.6.17a), but curve slightly downwards in the limit $k^2 \to 0$. These difficulties can be circumvented[34] by the introduction of another exponent, η, which allows

$h(r)$ for large r to be written as

$$h(r) \sim \frac{A \exp(-r/\xi)}{r^{\mathcal{D}-2+\eta}} \tag{5.6.20}$$

where $\mathcal{D}$ is the dimensionality; the Ornstein–Zernike approximation is recovered by putting $\eta = 0$. In the limit $\xi \to \infty$, the Fourier transform of (5.6.20) is

$$\hat{h}(k) \sim \frac{A}{k^{2-\eta}} \tag{5.6.21}$$

and a non-zero value of η can account for the non-linearity of the plots of $1/S(k)$ versus k^2. Substitution of (5.6.21) in the compressibility equation (2.6.12) yields a relation between the exponents γ, ν and η:

$$\nu(2-\eta) = \gamma \tag{5.6.22}$$

This result is independent of dimensionality. The value of η is difficult to determine experimentally, but the available evidence suggests that it is a small, positive number, approximately equal to 0.05.

5.7 SCALING CONCEPTS AND HIERARCHICAL REFERENCE THEORY

The shortcomings of mean-field theory in the critical region are linked to its inability to describe the onset of large-scale density fluctuations close to the critical point, where the correlation length ξ diverges. The scaling concepts introduced by Widom[36] and Kadanoff[37] in the 1960s, and later formalised by Wilson within renormalisation-group theory,[38] are ultimately based on the recognition that ξ is the only relevant length scale near criticality. The divergence of ξ as $T \to T_c$ causes the fluid to become "scale invariant", meaning that fluctuations on all length scales are self-similar; this in turn implies that critical behaviour is universal.

Scaling laws follow from an explicit assumption concerning the functional form of thermodynamic potentials near the critical point. The basic idea is perhaps most easily illustrated in the case of the chemical potential, which is the "ordering field" conjugate to the "order parameter" $(\rho_L - \rho_G)$. These two variables play roles analogous to the external field and magnetisation in the Ising model, which belongs to the same universality class as simple fluids. At the critical point we see from (2.4.21) and (5.6.5) that the chemical potential satisfies the conditions

$$\left(\frac{\partial \mu}{\partial \rho}\right)_{T=T_c} = \left(\frac{\partial^2 \mu}{\partial \rho^2}\right)_{T=T_c} = 0 \tag{5.7.1}$$

If μ is assumed to be an analytic function of ρ and T at the critical point, a Taylor expansion similar to (5.6.7) can be made. By introducing the reduced variables

$$\mu^* = \frac{\mu \rho_c}{P_c}, \qquad \Delta\rho^* = \frac{\rho - \rho_c}{\rho_c}, \qquad \Delta T^* = \frac{T - T_c}{T_c} \tag{5.7.2}$$

and taking account of (5.7.1), the result to first order in ΔT^* may be written as

$$\begin{aligned}\Delta\mu^* &= \mu^*(\rho, T) - \mu^*(\rho_c, T) \\ &\approx \frac{(\mu - \mu_c)\rho_c}{P_c} - \mu^*_{10}\Delta T^* \approx \mu^*_{11}\Delta\rho^*\Delta T^* + \mu^*_{03}(\Delta\rho^*)^3 \end{aligned} \tag{5.7.3}$$

where

$$\mu^*_{ij} = \left(\frac{\partial^{i+j}\mu^*}{\partial\Delta T^{*i}\,\partial\Delta\rho^{*j}}\right)_{\rho=\rho_c, T=T_c} \tag{5.7.4}$$

The classical values of the critical exponents are now easily recovered. In particular, since ΔT^* is zero along the critical isotherm:

$$\Delta\mu^* = \pm D^*|\Delta\rho^*|^\delta = D^*\Delta\rho^*|\Delta\rho^*|^{\delta-1} \tag{5.7.5}$$

where $\delta = 3$ and $D^* = \mu^*_{03}$. Similarly, because $\Delta\mu^*$ vanishes along the coexistence curve:

$$\Delta\rho^* = \pm B^*|\Delta T^*|^\beta \tag{5.7.6}$$

where $\beta = \frac{1}{2}$ and $B^* = (\mu^*_{11}/\mu^*_{03})^\beta$.

We now introduce a dimensionless *scaling parameter*, defined as

$$x = \Delta T^*/|\Delta\rho^*|^{1/\beta} \tag{5.7.7}$$

Clearly x is zero along the critical isotherm and is infinite along the critical isochore, while along the coexistence curve $x = -x_0 = -(B^*)^{1/\beta}$. Equation (5.7.3) can therefore be rewritten in generic form as

$$\Delta\mu^* = \Delta\rho^*|\Delta\rho^*|^{\delta-1}h(x) \tag{5.7.8}$$

where, in the classical theory:

$$h(x) = \mu^*_{03}(1 + x/x_0) \tag{5.7.9}$$

One way of formulating the scaling hypothesis is to postulate that non-classical critical behaviour still yields a result having the general form of (5.7.8), but with non-classical values of the exponents β and δ and a different (but unspecified) expression for $h(x)$, assumed to be an analytic function of x for $-x_0 < x < \infty$ and to vanish as $x \to x_0$.[39]

The scaling hypothesis leads to relations between the critical exponents, from which the values of all exponents can be obtained once two are specified. Consider, for example, the exponent γ', which describes the behaviour of the isothermal compressibility along the coexistence curve. Given that $x = -x_0$ and $h(x) = 0$, it follows from (5.7.6) and (5.7.8) that

$$\left(\frac{\partial\Delta\mu^*}{\partial\Delta\rho^*}\right)_{\Delta T^*} = -\frac{1}{\beta}|\Delta\rho^*|^{\delta-1-1/\beta}\Delta T^* h'(-x_0) \sim |\Delta T^*|^{\beta(\delta-1)} \tag{5.7.10}$$

where $h'(x) \equiv \mathrm{d}h(x)/\mathrm{d}x$. Then, since $\chi_T^{-1} = \rho^2(\partial\mu/\partial\rho)_T$ (see (2.4.22)), comparison with the definition of the exponent γ' in Table 5.1 shows that

$$\gamma' = \beta(\delta - 1) \tag{5.7.11}$$

In a similar way it is possible to establish the relations

$$\gamma = \gamma', \qquad \alpha' + 2\beta + \gamma' = 2, \qquad \alpha' + \beta(1 + \delta) = 2 \tag{5.7.12}$$

However, since this analysis rests on a hypothesis that refers only to thermodynamic quantities, it yields no information about the correlation-length exponents ν, ν' and η. Relations involving those quantities can be derived by exploiting scale invariance near the critical point within Kadanoff's "block-spin" construction for magnetic systems.[37] That approach leads back to the exponent relation (5.6.22) and to the "hyperscaling" relation, which involves the dimensionality $\mathcal{D}$ of the system:

$$\nu\mathcal{D} = 2 - \alpha \tag{5.7.13}$$

Although scaling arguments lead to relations between the critical exponents, they cannot be used to derive numerical values of the exponents given only the hamiltonian of the system. That goal can be reached within renormalisation-group theory, which is basically an iterative scheme whereby the total number of degrees of freedom contained in a volume of order $\xi^{\mathcal{D}}$ is systematically reduced to a smaller set of effective degrees of freedom. The reduction is brought about by successive elimination of fluctuations of wavelength $\lambda < L$, where the length L is progressively allowed to approach ξ. Scaling laws turn out to be a natural consequence of the theory. The set of transformations τ associated with the progressive reduction in the numbers of degrees of freedom gradually transforms a given initial hamiltonian, belonging to some universality class, into a fixed point of τ, i.e. a hamiltonian that is invariant under the transformation; the existence of a fixed point is equivalent to the principle of universality. The theory shows that for dimensionality $\mathcal{D} > 4$, fluctuations of wavelength λ become negligible as λ increases, and mean-field theory is therefore exact. Deviations from classical behaviour for $\mathcal{D} < 4$ can be expanded in powers of $\varepsilon = 4 - \mathcal{D}$ by the use of field-theoretic techniques; this allows the calculation of the non-classical exponents in three dimensions.[40]

Renormalisation-group ideas have been combined with those of thermodynamic perturbation theory in the hierarchical reference theory or HRT of Parola, Reatto and coworkers,[41] which leads to a non-classical description of criticality. The starting point of HRT is closely related to the treatment of long-range interactions in Section 5.5. We assume again that the total pair potential is divided into a repulsive, reference part, $v_0(r)$, and an attractive perturbation, $w(r)$. Then, in the random-phase approximation (5.5.13) and (5.5.29), the reduced free-energy density $\phi = -\beta F^{\mathrm{ex}}/V$ is given by

$$\begin{aligned}\phi = \phi_0 &+ \tfrac{1}{2}\rho^2 \int g_0(r)\Psi(r)\,\mathrm{d}\mathbf{r} \\ &- \tfrac{1}{2}(2\pi)^{-3} \int \left(\widehat{\Sigma}_0(k)\widehat{\Psi}(k) + \ln\left[1 - \widehat{\Sigma}_0(k)\widehat{\Psi}(k)\right]\right)\mathrm{d}\mathbf{k}\end{aligned} \tag{5.7.14}$$

where a subscript 0 denotes a property of the reference system, $\Psi(r) = -\beta w(r)$ and $\widehat{\Sigma}_0(k) = \rho S_0(k) = \rho^2/[1 - \rho\hat{c}_0(k)]$. Use of Parseval's relation allows (5.7.14) to be rewritten as

$$\phi = \phi_0 + \tfrac{1}{2}\rho^2 \int \Psi(r)\,\mathrm{d}\mathbf{r} - \tfrac{1}{2}(2\pi)^{-3} \int \big(\rho\widehat{\Psi}(k) + \ln\big[1 - \widehat{\Sigma}_0(k)\widehat{\Psi}(k)\big]\big)\,\mathrm{d}\mathbf{k} \qquad (5.7.15)$$

where the first two terms on the right-hand side correspond to the mean-field approximation (5.6.3) and the final term is the contribution made by fluctuations. The non-analyticities in the free energy that characterise the critical region mean, however, that a straightforward perturbative treatment of the effect of fluctuations is bound to fail. The renormalisation-group approach provides a hint of how to go beyond conventional perturbation theory. Density fluctuations must be introduced selectively and recursively, starting from short-wavelength fluctuations, which modify the local structure of the reference fluid, up to longer wavelengths, which eventually lead to condensation. The gradual switching on of fluctuations is brought about by passing from the reference-system pair potential to the full potential via an infinite sequence of intermediate potentials

$$v^{(Q)}(r) = v_0(r) + w^{(Q)}(r) \qquad (5.7.16)$$

where the perturbation $w^{(Q)}(r)$ contains only those Fourier components of $w(r)$ corresponding to wavenumbers $k > Q$. In other words:

$$\begin{aligned} \widehat{w}^{(Q)} &= \widehat{w}(k), \quad k > Q, \\ &= 0, \qquad k < Q \end{aligned}$$

and the reference-system and full potentials are recovered in the limits $Q \to \infty$ and $Q \to 0$, respectively:

$$\lim_{Q\to\infty} v^{(Q)}(r) = v_0(r), \qquad \lim_{Q\to 0} v^{(Q)}(r) = v(r) \qquad (5.7.17)$$

The "Q-system", i.e. the fluid with pair potential $v^{(Q)}(r)$, serves as the reference system for a fluid of particles interacting through the potential $v^{(Q-\delta Q)}(r)$, corresponding to an infinitesimally lower cut-off in $\mathbf{k}$-space. The parameter Q, like the inverse-range parameter γ in (5.5.3), has no microscopic significance; its role, as we shall see, is merely to generate a sequence of approximations that interpolate between the mean-field result and the exact solution for the fully interacting system.

The cut-off in $\widehat{w}(k)$ at $k = Q$ leads to discontinuities in the free energy and pair functions of the Q-system. To avoid the difficulties that this would create, a modified free-energy density $\bar{\phi}^{(Q)}$ is introduced, defined as

$$\bar{\phi}^{(Q)} = \phi^{(Q)} + \tfrac{1}{2}\rho^2\big[\widehat{\Psi}(0) - \widehat{\Psi}^{(Q)}(0)\big] - \tfrac{1}{2}\rho\big[\Psi(0) - \Psi^{(Q)}(0)\big] \qquad (5.7.18)$$

together with a modified direct correlation function $\widehat{\mathcal{C}}^{(Q)}$, given by

$$\widehat{\mathcal{C}}^{(Q)}(k) = \hat{c}^{(Q)}(k) - 1/\rho + \widehat{\Psi}(k) - \widehat{\Psi}^{(Q)}(k) \qquad (5.7.19)$$

where $c^{(Q)}(k)$ is the direct correlation function of the Q-system, defined in the usual way, and $\Psi^{(Q)}(r) = -\beta w^{(Q)}(r)$. Inclusion of the last two terms[42] on the right-hand side of (5.7.19) compensates for the discontinuity, equal to $\beta\widehat{w}(k)$, that appears in the function $\hat{c}^{(Q)}(k)$ at $k = Q$. Thus

$$\begin{aligned}\widehat{\mathcal{C}}^{(Q)}(k) &= -\frac{1}{\widehat{\Sigma}^{(Q)}(k)}, \qquad k > Q, \\ &= -\frac{1}{\widehat{\Sigma}^{(Q)}(k)} + \widehat{\Psi}(k), \quad k < Q\end{aligned} \tag{5.7.20}$$

with $\widehat{\Sigma}^{(Q)}(k) = \rho S^{(Q)}(k)$. With these definitions, the expression derived from (5.7.15) for $\bar{\phi}^{(Q-\delta Q)}$ in terms of $\bar{\phi}^{(Q)}$ can be written as

$$\bar{\phi}^{(Q-\delta Q)} = \bar{\phi}^{(Q)} + \tfrac{1}{2}(2\pi)^{-3}\int \ln\left(1 - \frac{\widehat{\Psi}(k)}{\widehat{\mathcal{C}}^{(Q)}(k)}\right)\mathrm{d}\mathbf{k} \tag{5.7.21}$$

where the integration is confined to the interval $Q - \delta Q < k < Q$. By taking the limit $\delta Q = 0$ we arrive at an exact, differential equation for $\bar{\phi}^{(Q)}$, which describes the evolution of the free energy with Q:

$$-\frac{\mathrm{d}\bar{\phi}^{(Q)}}{\mathrm{d}Q} = \frac{Q^2}{4\pi^2}\ln\left(1 - \frac{\widehat{\Psi}(Q)}{\widehat{\mathcal{C}}^{(Q)}(Q)}\right) \tag{5.7.22}$$

The initial condition is imposed at $Q = \infty$, where the free energy takes its mean-field value, i.e.

$$\phi^{(\infty)} = \phi_0 + \tfrac{1}{2}\rho^2\widehat{\Psi}(0) - \tfrac{1}{2}\rho\Psi(0) \tag{5.7.23}$$

or, equivalently, $\bar{\phi}^{(\infty)} = \phi_0$.

Methods similar to those sketched above can be used to derive a formally exact, infinite hierarchy of differential equations that link the pair function $\mathcal{C}^{(Q)}(k)$ to all higher-order direct correlation functions $\hat{c}_n^{(Q)}(\mathbf{r}_1, \ldots, \mathbf{r}_n)$, $n \geqslant 3$. Close to the critical point some simplification occurs at small values of Q, i.e. when critical fluctuations begin to make a contribution to the free energy. The definitions (5.7.18) and (5.7.19) imply that a generalisation of the compressibility relation (3.5.15):

$$\widehat{\mathcal{C}}^{(Q)}(k=0) = -\frac{\partial^2\bar{\phi}^{(Q)}}{\partial\rho^2} \tag{5.7.24}$$

applies for all Q. The resulting divergence of $1/\widehat{\mathcal{C}}^{(Q)}(k)$ in the limit $k \to 0$ means that the argument of the logarithmic function in (5.7.21) is dominated by the term describing pair correlations. Thus the evolution of the free energy with Q in its final stages has a universal character, being essentially independent of the interaction term $\widehat{\Psi}(k)$. Similar simplifications appear at all levels of the hierarchy, and the distinctive features of renormalisation-group theory, such as scaling laws and the expansion in powers of $\varepsilon = 4 - \mathcal{D}$, emerge

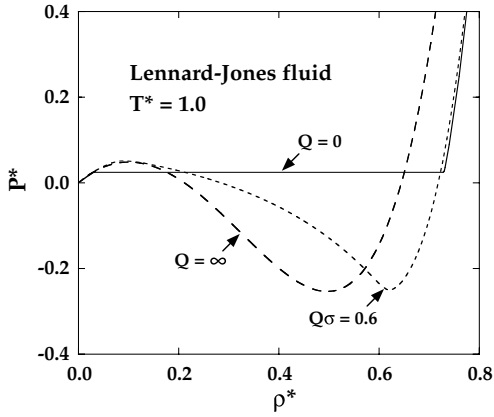

FIG. 5.9. An isotherm of the Lennard-Jones fluid in the pressure–density plane, calculated at three different stages in the integration of (5.7.22); $P^* = P\sigma^3/\varepsilon$ is the reduced pressure. The limits $Q = \infty$ and $Q = 0$ correspond, respectively, to the mean-field and final solutions. For $Q = 0$ the theory yields an isotherm that is rigorously flat in the two-phase region, while at finite Q van der Waals loops are obtained.

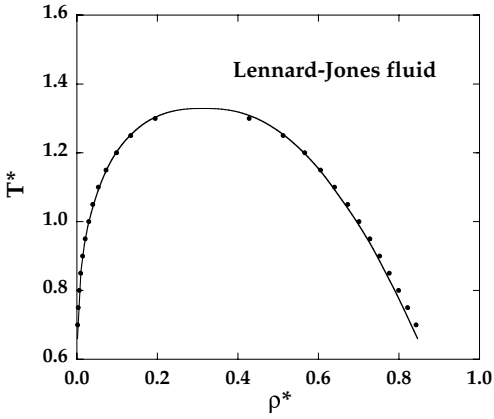

FIG. 5.10. Liquid–vapour coexistence curve for the Lennard-Jones fluid. The curve is calculated from HRT and the points are the results of Monte Carlo calculations.[45] After Tau *et al.*[43]

from the formalism without recourse to field-theoretical models. Away from the critical region some approximate closure of the hierarchy is required if numerical results are to be obtained. In practice this is achieved at the level of the free energy by approximating the function $\widehat{\mathcal{C}}^{(Q)}(k)$ in a form that is consistent both with (5.7.24) and with the Ornstein–Zernike assumption that $\widehat{\mathcal{C}}^{(Q)}(k)$ is analytic in k^2 (see (5.6.17)). The first equation of the hierarchy is thereby transformed into a partial differential equation in the variables Q and ρ. Closures of this general type, having features in common with other approximate theories, have been used in calculations for a variety of simple fluids.[43,44] Overall the theory yields a very satisfactory description of liquid–vapour coexistence. Non-classical values

are obtained for the critical exponents, though these differ somewhat from the nearly exact results derived from the ε expansion.[41(b)] For example, within HRT, $\beta \approx 0.345$, while the ε expansion gives $\beta \approx 0.327$. Below T_c the theory leads to rigorously flat isotherms in the two-phase region, illustrated by the results for the Lennard-Jones fluid shown in Figure 5.9. The coexistence curve can therefore be determined without use of the Maxwell construction, with results in excellent agreement with those obtained by simulation, as Figure 5.10 reveals. A fault in the theory is the fact that it leads to an artificial divergence of the isothermal compressibility along the coexistence curve, which therefore coincides with the spinodal everywhere, not just at the critical point (cf. Figure 5.8). The source of this error is the analyticity imposed on $\widehat{\mathcal{C}}^{(Q)}(k)$.

NOTES AND REFERENCES

1. Widom, B., *J. Chem. Phys.* **39**, 2808 (1963).
2. Longuet-Higgins, H.C. and Widom, B., *Mol. Phys.* **8**, 549 (1964).
3. Ashcroft, N.W. and Lekner, J., *Phys. Rev.* **145**, 83 (1966).
4. Verlet, L., *Phys. Rev.* **163**, 201 (1968).
5. Zwanzig, R., *J. Chem. Phys.* **22**, 1420 (1954).
6. Henderson, D. and Barker, J.A., *In* "Physical Chemistry: An Advanced Treatise", vol. VIIIA (H. Eyring, D. Henderson and W. Jost, eds). Academic Press, New York, 1971.
7. Isihara, A., *J. Phys. A* **1**, 539 (1968).
8. (a) Mansoori, G.A. and Canfield, F.B., *J. Chem. Phys.* **51**, 4958 (1969). (b) Rasaiah, J.C. and Stell, G., *Mol. Phys.* **18**, 249 (1970).
9. Ben-Amotz, D. and Stell, G., *J. Chem. Phys.* **120**, 4844 (2004).
10. (a) Mon, K.K., *J. Chem. Phys.* **112**, 3245 (2000). (b) Mon, K.K., *J. Chem. Phys.* **115**, 4766 (2001).
11. Andersen, H.C., Weeks, J.D. and Chandler, D., *Phys. Rev. A* **4**, 1597 (1971).
12. Rowlinson, J.S., *Mol. Phys.* **8**, 107 (1964).
13. Barker, J.A. and Henderson, D., *J. Chem. Phys.* **47**, 4714 (1967).
14. Hansen, J.P. and Weis, J.J., *Mol. Phys.* **23**, 853 (1972).
15. Lado, F., *Mol. Phys.* **52**, 871 (1984). See also Ben-Amotz, D. and Stell, G., *J. Phys. Chem. B* **108**, 6877 (2004).
16. (a) Levesque, D. and Verlet, L., *Phys. Rev.* **182**, 307 (1969). (b) Verlet, L. and Weis, J.J., *Mol. Phys.* **24**, 1013 (1972).
17. McQuarrie, D.A. and Katz, J.L., *J. Chem. Phys.* **44**, 2398 (1966).
18. Barker, J.A. and Henderson, D., *Rev. Mod. Phys.* **48**, 587 (1976).
19. Weeks, J.D., Chandler, D. and Andersen, H.C., *J. Chem. Phys.* **54**, 5237 (1971).
20. Talbot, J., Lebowitz, J.L., Waisman, E.M., Levesque, D. and Weis, J.J., *J. Chem. Phys.* **85**, 2187 (1986).
21. (a) Hemmer, P.C., *J. Math. Phys.* **5**, 75 (1964). (b) Lebowitz, J.L., Stell, G. and Baer, S., *J. Math. Phys.* **6**, 1282 (1965).
22. Kac, M., Uhlenbeck, G.E. and Hemmer, P.C., *J. Math. Phys.* **4**, 216 (1963). For the extension to three dimensions, see van Kampen, N.G., *Phys. Rev.* **135**, 362 (1964) and Lebowitz, J.L. and Penrose, O., *J. Math. Phys.* **7**, 98 (1966).
23. Andersen, H.C. and Chandler, D., *J. Chem. Phys.* **57**, 1918 (1972).
24. Except in trivial cases, removal of a reference articulation pair causes a diagram to separate into two or more components, of which at least one contains only reference-system bonds.
25. See, e.g., Tables VIII and IX of ref. 18.
26. Pini, D., Parola, A. and Reatto, L., *Mol. Phys.* **100**, 1507 (2002).
27. For a discussion of the relationship between the two expansions, see Stell, G., *J. Chem. Phys.* **55**, 1485 (1971).
28. Stell, G. and Weis, J.J., *Phys. Rev. A* **21**, 645 (1980).
29. See, e.g., Caccamo, C., *Phys. Rep.* **274**, 1 (1996).

30. Huang, K., “Statistical Mechanics”, 2nd edn. John Wiley, New York, 1987, p. 41.
31. Alder, B.J., Young, D.A. and Mark, M.A., *J. Chem. Phys.* **56**, 3013 (1972).
32. (a) Rowlinson, J.S. and Swinton, F.L., “Liquids and Liquid Mixtures”, 3rd edn. Butterworth, London, 1982. (b) Chaikin, P.M. and Lubensky, T.C., “Principles of Condensed Matter Physics”. Cambridge University Press, Cambridge, 1995.
33. Note that the prefactors (the critical amplitudes) that appear in the scaling laws are not universal quantities.
34. Fisher, M.E., *J. Math. Phys.* **5**, 944 (1964).
35. See, e.g., Ferrenberg, A.M. and Landau, D.P., *Phys. Rev. B* **44**, 5081 (1991) (Ising model) and Wilding, N.B., *Phys. Rev. E* **52**, 602 (1995) (Lennard-Jones fluid).
36. Widom, B., *J. Chem. Phys.* **43**, 3898 (1965).
37. (a) Kadanoff, L.P., *Physics* **2**, 263 (1966). (b) Kadanoff, L.P., “Statistical Physics: Statics, Dynamics and Renormalization”. World Scientific, Singapore, 1999.
38. (a) Wilson, K.G., *Phys. Rev. B* **4**, 3174 and 3184 (1971). (b) Fisher, M.E., *Rev. Mod. Phys.* **70**, 653 (1998). For introductory treatments, see the book by Huang, ref. 30, and Plischke, M. and Bergersen, B., “Equilibrium Statistical Physics”, 2nd edn. World Scientific, Singapore, 1994.
39. Griffiths, R.B., *Phys. Rev.* **158**, 176 (1967).
40. (a) Wilson, K.G. and Kogut, J., *Phys. Rep.* **12**, 75 (1974). (b) Amit, D.J., “Field Theory, the Renormalization Group and Critical Phenomena”, 2nd edn. World Scientific, Singapore, 1993.
41. (a) Parola, A. and Reatto, L., *Phys. Rev. A* **31**, 3309 (1985). (b) Parola, A. and Reatto, L., *Adv. Phys.* **44**, 211 (1995).
42. The second term is introduced in order to simplify the resulting expressions.
43. See, e.g., Tau, M., Parola, A., Pini, D. and Reatto, L., *Phys. Rev. E* **52**, 2644 (1995). For a description of the numerical implementation, see Reiner, A. and Kahl, G., *Phys. Rev. E* **65**, 046701 (2002).
44. HRT has also been successfully generalised to binary systems. See, e.g., Pini, D., Tau, M., Parola, A. and Reatto, L., *Phys. Rev. E* **67**, 046116 (2003).
45. Lotfi, A., Vrabec, J. and Fischer, J., *Mol. Phys.* **76**, 1319 (1992).